CHRISTOPHER MICHAEL MODLESKY

Trabecular Bone Microarchitecture, Bone Geometric Structure and Skeletal Muscle in Men with Spinal Cord Injury

(Under the direction of KIRK J. CURETON and GARY A. DUDLEY)

The primary purpose of these studies was to determine if men with spinal cord injury (SCI) have lower trabecular bone microarchitecture about the knee and impaired bone geometric structure and strength in the mid-thigh relative to controls. A secondary purpose was to assess the degree of muscle atrophy using magnetic resonance imaging and dual-energy X-ray absorptiometry. Magnetic resonance images were used to assess bone in the lower limbs, and to quantify skeletal muscle mass in the mid-thigh. Dual-energy X-ray absorptiometry was used to quantify fat-free soft tissue mass (FFST) in the mid-thigh.

The distal femur and proximal tibia of men with SCI had fewer trabeculae (21 and 19 %) that were further apart (43 and 32 %) than controls, resulting in less bone per unit volume after injury (26 and 18 %). In addition, within a small area of the proximal tibia (~3 cm), the volume and number of trabeculae decreased from the most proximal end to the most distal end in the SCI group than controls while the opposite was the case for spacing. Differences in microarchitecture between groups along the length of the femur, in contrast, were consistent.

Total volume of the mid-femur was not different and total width only modestly thinner (3 to 6%) in the SCI group than controls, but cortical volume and width were 22 to 39 % less in the SCI group. The cortical wall was particularly thin and the endosteum

particularly thick in the posterior region. Congruent with the structural deterioration, bone strength was reduced by 15 to 35 %.

With respect to skeletal muscle, the SCI group had lower muscle mass (45 %) and FFST (38 %) in the mid-thigh than controls; however, skeletal muscle was disproportionately lower, as indicated by the lower proportion of muscle in the FFST of the SCI group (80 % vs 91 %, respectively; $P < 0.05$). Despite the latter discrepancy, strong relationships were observed between mid-thigh skeletal muscle and FFST in the SCI men and controls ($r = 0.99$ and 0.96, respectively; $P < 0.05$).

These studies suggest that trabecular bone microarchitecture and bone geometric structure deteriorates to a great extent in the lower limbs after SCI. Moreover, they suggest that SCI results in a disproportionately lower concentration of skeletal muscle in the FFST.

INDEX WORDS: Trabecular bone microarchitecture, bone geometry, bone quality, spinal cord inury, magnetic resonance imaging, skeletal muscle

# TRABECULAR BONE MICROARCHITECTURE, BONE GEOMETRIC STRUCTURE AND SKELETAL MUSCLE IN MEN WITH SPINAL CORD INJURY

by

CHRISTOPHER MICHAEL MODLESKY

B.S., State University of New York College at Cortland, 1992

M.A., The University of Georgia, 1995

A Dissertation Submitted to the Graduate Faculty of The University of Georgia in Partial Fulfillment of the Requirements for the Degree

DOCTOR OF PHILOSOPHY

ATHENS, GEORGIA

August 2002

TRABECULAR BONE MICROARCHITECTURE, BONE GEOMETRIC

STRUCTURE AND SKELETAL MUSCLE IN MEN WITH SPINAL CORD INJURY

by

CHRISTOPHER MICHAEL MODLESKY

Approved:

Major Professor Kirk J. Cureton
Gary A. Dudley

Committee

Ronald Elliott
Richard D. Lewis
Kevin K. McCully
Patrick J. O'Connor

Electronic Version Approved:

Gordham L. Patel
Dean of the Graduate School
The University of Georgia
August 2002

DEDICATION

Dr Gary A. Dudley

ACKNOWLEDGEMENTS

Several individuals made the completion of this project possible. I would like to express my gratitude to the following:

Dr Gary Dudley, for providing me with your wisdom and guidance throughout this rigorous process. You have carved out an exciting line of research, the true impact of which has yet to be realized. Thank you for allowing me to be a part of such an endeavor.

Dr Kirk Cureton, for your continued support throughout my graduate education. You have unselfishly given of your time and have always provided excellent direction. Your unique combination of patience and leadership has benefited all students who have passed through the Department of Exercise Science at The University of Georgia.

Dr Richard Lewis, for your friendship and support during the past eight years. You have shown me the importance of balance between family, career and leisure. I will always remember our collaborative efforts, the late nights of grant writing, the memorable five o'clock drive to Mailboxes Plus and the nutritious lab meetings at Steverino's and Hodgson's Drug Store.

Dr Sharmila Majumdar for sharing your ideas and work with us. You have allowed us to move into an exciting new direction. I hope this is the beginning of a long and fruitful relationship.

Dr Patrick O'Connor, for our late afternoon discussions about research, statistics and life. I'll never forget your clever dance steps at the wedding of Dane and Karen Cook.

Dr Ronald Elliott, for your unselfish participation during the completion of this project as well as providing a sound clinical perspective.

Dr Kevin McCully, for your thought provoking questions and insight into magnetic resonance imaging and muscle physiology. I thank you for stepping during the final leg of the project to make its completion possible.

Jill Slade, for your excellent support during the final months of this project. You were a pleasure to work with and will be an excellent addition to bone and exercise community.

Scott Bickel, for your unselfish assistance during the initial stages of the study and your continued support throughout the project.

Marlee Stewart, for always being on the ball and going the extra mile to help out. You are the heart of the Department of Exercise Science. Chase thanks you and Donna Smith for "fussing over him" and making him feel like a part of the Department.

Donna Smith, for helping out during times of need.

Chris Elder, for taking the time to share your knowledge about image analysis. Your attention to detail and quest for the "right answer" will serve you well in your future endeavors.

Ashrof Gorgey, for always stepping forward to lend a hand. I wish you and your family well during your stay in the United States.

Emma Laing, for your continued encouragement and support during this process. You are an excellent leader and will be an exceptional academician.

Anna Kate Hein, for playing with Chase during crunch time.

Barry and Anita Bunn, for providing us with a family away from home.

All family members and friends, for supporting Debbie and I during this venture.

Chase, my son, for making me laugh and for hanging on a few extra minutes in the morning so I could get one complete hour of sleep during each of the final days of the project.

Finally, I thank Debbie, my wife, for your encouragement, support, love and understanding. Without your help, the completion of this project would have been impossible and much less meaningful.

TABLE OF CONTENTS

# Chapter I

## INTRODUCTION

Spinal cord injury (SCI) affects 183,000 to 238,000 people in the U.S. with more than 10,000 new injuries annually (36). Complete SCI is the most severe form resulting in a loss of all sensation (ascending tracts severed) and motor function (descending tracts severed) more than three neurologic segments below the level of injury (36). The loss of motor function and the inability to ambulate results in a rapid decrement in areal bone mineral density (aBMD) and bone mineral content (BMC) (7, 8, 50) and parallel declines in skeletal muscle (96) below the level of injury. In paraplegics, the deterioration of bone and skeletal muscle occur almost exclusively in the lower extremities.

The bone decrement is striking (7, 8, 50). Decreases in lower limb aBMD and BMC are approximately 1.5 to 2 %/month during the first 3 to 12 months following injury (110). A steady state is reached at approximately 2 years after injury, at which time BMC is 40 to 50 % of normal in the proximal tibia and 60-70 % of normal in the femoral neck (8). Trabecular bone is most affected (8, 22), with rates of loss of 4 to 5 %/month being reported (73, 74, 110). The pattern of bone loss is consistent with the dramatic increase in lower limb fractures.

Although aBMD is currently the best *in vivo* surrogate of fracture risk widely available, explaining 60 to 80% of the variance in bone strength (12, 100), there is substantial overlap in those who do and do not experience skeletal fracture. It has been

hypothesized that the unexplained variability is due to other components of bone, such as microarchitecture of trabecular bone and geometric structure of bone shafts (17, 24, 55, 61, 67, 82). This notion is supported by studies demonstrating an improvement in the prediction of strength and fracture when bone mineral measures are combined with trabecular bone microarchitecture (67) or bone geometry (29).

Despite the high incidence of fracture about the knee after SCI and the high concentration of trabecular bone in the distal femur and proximal tibia, the microarchitecture of trabecular bone in this region has not been investigated. The paucity of studies can be attributed to limited technology. Fortunately, advances in the application of high resolution MRI now make it feasible to conduct previously impossible studies of human trabecular microarchitecture. Studies conducted in lower mammals have demonstrated impaired connectivity of trabecular bone following relatively short periods (one or more weeks) of unloading (10, 105). If a similar response is exhibited in humans, rapid and dramatic deterioration of trabecular bone microarchitecture can be expected in individuals with SCI. Determining if trabecular bone microarchitecture is impaired in individuals with SCI is important because loss of structural connectivity appears to be an irreversible process (82). New lamellar bone can only be added to existing surfaces, thus, loss of trabecular microstructure can have serious implications, even if aBMD can be restored with intervention strategies (82).

A handful of studies have attempted to quantify the geometric structure and strength of the femoral and tibial shafts in individuals with SCI. These studies suggest there is no change in the size of the bone, but there is a marked deterioration of its internal structure (21, 52, 56). Thinner cortical walls and expanded medullary cavities

have been noted. While these studies unanimously agree that SCI is associated with structural deterioration of the long bones, its affect on bone strength is less clear. One (54) of the three (21, 52, 56) studies suggests bone strength is not adversely affected by SCI and another (56) suggests the modulus of elasticity but not the polar moment of inertia (J) is affected by SCI. These findings, however, are inconsistent with the structural deterioration known to occur following this debilitating injury. Moreover, they are incongruent with the marked increase in fracture incidence in the lower limbs after injury (20, 31). The inconsistency may be related to the age and health of the subjects as well as the methodologies employed. In the study by Lee et al. (58), the subjects were elderly and suffering from peripheral vascular disease. In the study by Kiratli et al. (54), radiography was used to assess the geometric structure of bone. The considerable variability associated with radiography (40) may limit its usefulness in the assessment of bone structure. Studying young healthy subjects with SCI and using methodologies that provide a reliable three-dimensional (3D) visualization of bone, such as magnetic resonance imaging (MRI), may give some better insight into the changes in long bone structure and strength induced by extreme unloading of the skeleton.

The usefulness of MRI in understanding the degree of tissue deterioration following SCI is certainly not limited to bone. Studies employing MRI have demonstrated a severe deterioration of skeletal muscle after SCI. However, because of the limited availability of MRI, determining if more accessible methods, such as dual-energy X-ray absorptiometry (DXA), provide valid estimates of skeletal muscle in individuals with severe atrophy is worthwhile. It is often assumed that skeletal muscle represents a certain proportion or all of the fat-free soft tissue (FFST). Whether this

assumption is accurate in men with long-standing SCI is not known. However, a recent study in men and women with AIDS suggests the proportion of skeletal muscle in the adipose tissue-free mass of individuals with severe muscle wasting is lower than normal (106). If a similar phenomenon were exhibited in men with SCI it would suggest that estimates of skeletal muscle from DXA FFST underestimate the degree of atrophy in individuals with SCI. If so, this could limit the validity of DXA to assess skeletal muscle change induced by injury or intervention.

## Specific Aims

The specific aims of the projects were to determine if men with long-standing SCI have:

1) impaired trabecular bone microarchitecture about the knee,

2) deteriorated macroarchitecture, or structure, in the mid-shaft of the femur,

3) lower bone strength in the mid-shaft of the femur, and

4) a lower proportion of skeletal muscle relative to FFST in the mid-thigh

## Hypotheses

It is hypothesized that men with long-standing SCI have:

1) impaired trabecular bone microarchitecture about the knee,

2) deteriorated structure in the mid-shaft of the femur,

3) lower bone strength in the mid-shaft of the femur, and

4) a lower proportion of skeletal muscle relative to FFST in the mid-thigh

## Significance of the Study

If it is determined that the trabecular bone microarchitecture, bone geometric structure and calculated strength of bone in the lower limbs are impaired in men with SCI, then individuals with this debilitating condition may be at higher risk of fracture in the lower limbs than indicated by aBMD alone. Such a finding would further support the need to identify intervention strategies that would reduce the loss of bone following SCI. In theory, loss of trabecular bone microarechitecture cannot be regained; thus preventing such an occurrence would be commendable. If it is determined that skeletal muscle represents a smaller proportion of the FFST in the mid-thigh than controls, it would suggest that estimates of skeletal muscle in the lower limbs from DXA underestimate the degree of atrophy caused by SCI. Subsequently, models that estimate skeletal muscle using DXA would need to be adjusted for individuals with SCI or other conditions associated with extreme muscle atrophy.

## Limitations of the Study

Because of the cross-sectional design of the study, it is possible that any differences in bone between paraplegics and able-bodied controls may have been present prior to SCI. To minimize this problem, controls of similar age, height and weight, factors that may affect bone status, were recruited.

# Chapter II

## REVIEW OF THE LITERATURE

In this chapter, the following areas will be reviewed: 1) assessment of trabecular microarchitecture and geometric structure of bone using magnetic resonance imaging (MRI), 2) bone deterioration after spinal cord injury (SCI), 3) potential mechanisms underlying bone deterioration after SCI, 4) assessment of skeletal muscle using MRI, and 5) skeletal muscle deterioration after SCI.

### Assessment of Trabecular Microarchitecture and Geometric Structure of Bone Using MRI

Several *in vivo* methods have been developed in an attempt to quantify the status of the human skeleton. These methods range in sophistication from anthromopometry, which relies on simple measurements of body segments combined with assumptions about the proportionality about different tissues, to MRI, in which an unparalleled visualization and quantification of the human body tissue is made possible. Because of its ability to delineated discrete parts of human anatomy, MRI is a powerful research tool used to study the morphology of different tissues and their response to adverse and favorable conditions.

*Quantification of Trabecular Bone Microarchitecture*

There are different aspects of trabecular bone that reflect its architectural properties. Standard bone histomorphometric measures include the bone fraction (BV/TV) or the volume of trabecular bone (BV) per total volume of the region of interest (TV), trabecular number (Tb.N), trabecular thickness (Tb.Th) and trabecular separation (Tb.Sp) (81, 83). Together, these measures reflect the quality of the trabecular component of the bone under study. Traditionally, trabecular bone microarchitecture has been quantified using two-dimensional histomorphometric sections obtained from the iliac crest. However, because of the invasiveness of the biopsy procedure and the limited number of sites that can be assessed, researchers have turned to *in vivo* methodologies (66). Recent developments with high resolution computed tomography and MRI now allow for 3D quantification of trabecular bone microarchitecture that is more flexible (ie, more bone sites can be assessed) and non-invasive. MRI is particularly useful in human studies because it does not expose individuals to high doses of radiation. Imaging procedures have been developed for quantification of trabecular bone microarchitecture in the distal radius (62), calcaneus (61, 78) and the knee (distal femur and proximal tibia) (6).

A general description of the procedure used to assess trabecular bone microarchitecture *in vivo* using MRI follows (64). The first step is to acquire high-resolution images with an in plane resolution between 78 μm and 200 μm and a slice thickness of 300 μm to 1000 μm. Factors that must be considered in the image acquisition include the sequence used (ie, gradient vs spin echo), echo time (TE), repetition time (TR) and bandwidth (64). Spin echo sequences use a 180 degree

radiofrequency pulse to obtain an echo signal which is used to acquire the image. With a gradient echo sequence, a reversal of magnetic field gradient is used to generate an echo. Both sequences result in an overestimation of trabecular dimensions (primarily Tb.Th and BV/TV), which is more pronounced with the gradient echo sequence (68). However, this overestimation is blunted when a short TE is used. Moreover, recent improvements in gradient strength of clinical imagers allows for high resolution image acquisition using a short TE. The advantage of the gradient echo sequence is that it can be used to acquire images *in vivo*. Because the TR affects the signal to noise ratio achievable, it must be considered carefully. While a higher TR increases the signal to noise ratio, it also increases the scan time. The signal to noise ratio is also affected by the bandwidth selected, or the total time the MR image is sampled. A higher bandwidth reduces the TE, but also reduces the signal to noise ratio. Hence, the intricate interplay between the sequence, TE, TR and bandwidth and their intricate interplay must be considered when choosing an imaging protocol.

Once the images are acquired, they are analyzed for the different microarchitectural components using a series of steps described by Goulet et al. (39). The first step is to apply an adaptive thresholding procedure to divide the image into bone and non-bone voxels. The chosen thresholding procedure accounts for varying densities of trabeculae encountered throughout the image. The bone fraction is determined based on the number of voxels with signal intensities below the bone threshold ($P_P$). The rest is categorized as non-bone (ie, marrow). The Tb.N is determined by superimposing a set of parallel lines over the region of interest and calculating the number of intersections between bone and nonbone components divided by the length of the test lines applied to

the region of interest ($P_L$). Since trabecular bone is anistropic, a single set of parallel lines would not give an accurate estimate of Tb.N. Instead, the grid of test lines is continually rotated by a set angle (5 degrees) and the same principle is applied at each rotation until the grid is fully rotated.

A major limitation of the procedure is that the size of pixels used to discriminate bone from marrow *in vivo* (78 to 200 μm) is often the size of the trabeculae being studied. This subjects the pixels to partial volume effects, such that most pixels contain some bone and some fat. To combat the problem, special methods have been developed in an attempt to quantify bone and marrow. For instance, Majumdar et al (65) have developed the following procedure. First, the signal intensity of the entire region of interest is determined ($I_r$). Then the histogram of pixel signal intensity vs pixel number is plotted. Next, the peak pixel signal intensity (ie, the most frequently occurring signal intensity) is identified. Because the peak intensity is a mixture of bone and marrow, its signal intensity should be higher than bone but lower than marrow. Then the marrow equivalent is set at the half way point between the lowest signal intensity and the peak signal intensity ($I_L$). Apparent BV/TV is then determined using a modification of the following equation:

$$I_r = (appBV/TV)I_b + (1 - appBV/TV)I_L.$$

.

with $I_b$ equal to the signal intensity of cortical bone surrounding the trabecular region of interest. Although the procedure has limitations, it has the ability to discriminate between those who and do not experience skeletal fracture (65).

The validity of trabecular bone microarchitecture has been demonstrated by assessing samples from different bones, such as the calcaneus, distal femur, proximal femur and vertebral bodies and comparing the measures against standard methodologies. Hipp et al. (44) compared MRI derived sterology measures of bovine trabecular bone with measures obtained using optical imaging. The ratio of trabecular bone volume to total volume and Tb.N from the two methods correlated strongly ($R^2$ = 0.81 and 0.53, respectively) and their absolute values were not statistically different (P > 0.05). Similarly, Chung et al. (16) found BV/TV from MRI to correlate well with measures using displacement methods.

Majumdar et al (69) compared trabecular bone microarchitecture measures quantified using MR images of the calcaneus, distal femur, proximal femur and vertebral bodies of human cadavers (spatial resolution = 156 x 156 x 300 μm) against XTM images using a standard clinical analyzer and a spatial resolution varying from 18 x 18 x 18 μm to 156 x 156 x 300 μm. Although the absolute numbers were markedly higher for BV/TV (~3 x) and Tb.Th (~1.6 x) and lower for Tb.Sp (~1.6 x) using MRI, architectural parameters from the two methods were moderately to highly correlated (r = 0.51 to 0.87). In a more recent study, Majumdar's group assessed the ability of MRI-derived trabecular bone microarchitecture measures to discriminate between those who have experienced a recent hip fracture vs non-fracture subjects. Although hip aBMD was a better discriminator than most microarchitectural parameters (area under the curve = 0.73 for total hip aBMD), apparent Tb.N of the distal radius showed a similar ability to discriminate between groups (area under the curve = 0.69). Furthermore, the

discrimination between fracture and non-fracture subjects was improved when hip aBMD and architectural measures were combined (area under the curve = 0.87).

Together, these studies support the validity of *in vivo* trabecular bone microarchitecture measures from MRI and suggest they can compliment bone mineral measures to improve the prediction of fracture risk.

*Quantification of Bone Structure and Strength*

Other procedures that can be conducted to gain a more complete understanding of the biologic changes that occur following SCI include quantification of the size, shape, cortical thickness, CSA and volume of the shafts of long bones in the lower limbs. These structural, or macroarchitectural, features are highlighted in Figure 2.1. Structural information can also be used to assess the strength of the long bones. Strength measures, such as cross-sectional moment of inertia (CSMI), polar moment of inertia (J) and polar section modulus (Z), can be estimated using the width of the total shaft of the bone and the width of the shaft's cortical walls. These strength measures reflect the long bones resistance to bending and have been employed in a handful of recent studies (27, 84)**.** Below are equations or adaptations of equations that have been developed to estimate bending and torsional strength (53, 101):

$$CSMI = \pi/4\ (TW^4 - (EW^4)$$

$$J = 2\pi\ (TW^4 - EW^4)/64$$

$$Z = J/(0.5*TW)$$

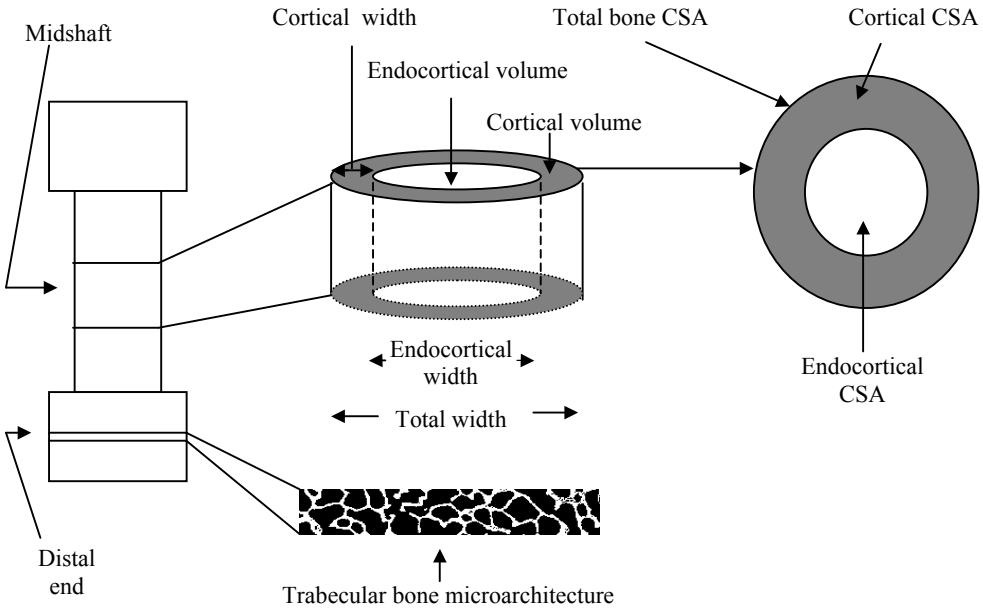


Figure 2.1. Trabecular microarchitecture and geometric structure of a long bone. From: Modlesky, C.M. and Lewis, R.D. Does exercise during growth have a long-term effect on bone? Exerc Sports Sci Rev (in Press).

in which TW is the width of the endocortical space.

Structural measures can also be combined with BMC from DXA to determine the volumetric BMD (vBMD) and cortical vBMD of long bones. Volumetric BMD, which describes the mineral portion of the bone relative to its total volume, has been shown to be a better predictor of fracture risk than aBMD (4). Therefore, it is regarded as a useful indicator of fracture risk. Volumetric BMD can be calculated using the following equation:

$$vBMD = BMC/TV$$

Cortical vBMD describes the mineral density of the shafts of the cortical walls. It can be determined by dividing BMC by CV.

$$\text{cortical vBMD} = BMC/CV$$

Another important strength measure recently introduced is the bone strength index (BSI) (29). The BSI was designed to reflect the combined influences of the mineral and biomechanical properties of bone. BSI can be determined using the following equation:

$$BSI = \text{cortical vBMD} \times CSMI$$

The potential value of the BSI was demonstrated in a study by Ferretti et al (29). Five week old Wistar rats (n = 103) were given doses of dexamethasone ranging from 0 to 1000 μg/kg body wt/day for 4 weeks or different doses of $Al(OH_3)$ (0 or 80 mg/kg

body wt/day) 3 x/week from 4 to 10 months of age. Cortical vBMD and CSMI were assessed using peripheral quantitative computed tomography (pQCT) and breaking force was assessed using three point bending. Dexmathasone treated rats were found to have a dose related reduction in breaking force, CSMI and cortical vBMD, whereas $Al(OH_3)$ treatment reduced breaking force and cortical vBMD, but increased CSMI. As a result of the different treatments there was wide range of values for all variables. BSI was more strongly correlated with breaking force ($r = 0.784$ and 0.896 for dexamethasone and $Al(OH_3)$ treated rats, respectively) than the other strength measures ($r = 0.413$ to 0.832). Moreover, BSI was a better correlate of fracture load than aBMD from DXA ($r = 0.198$ and 0.477 for dexamethasone and $Al(OH_3)$ treated rats, respectively) (29).

The validity of structural measures of the middle-femur using MRI was recently assessed in three venison femora and in custom-made Perspex cylindrical phantoms (111). Specific measures included TW, cortical width (CW), MW and CSA of the total (TCSA), cortical (CCSA) and medullary cavity (MCSA) regions of a single slice (6 mm thick) at the midpoint of the femur. Total and cortical volumes of three venison femora were assessed for the entire mid-femur by water displacement and by MRI. TW, CW, TCSA and CCSA were assessed using vernier calipers and MRI. MW and MCSA were determined by subtraction (total bone minus cortical bone). The phantoms were of known size that varied in diameter and thickness. The volumes and CSAs were calculated and confirmed by water displacement. The lengths of the phantoms were determined using vernier calipers. Measurements of the venison bones were made 5 times using MRI and the average used for comparison against the caliper and water displacement values (gold standards).

When the MRI and gold standard measures were compared for the three venison bones, TV, CV, TCSA and CCSA were not different between methods, but TW and CW measured by MRI (28.2 ± 0.9 mm and 3.9 ± 0.4 mm, respectively) were lower ($P < 0.05$) than the caliper measures (29.4 ± 1.1mm and 4.7 ± 0.2 mm, respectively). When MRI and the gold standard measures were compared for the phantoms, there were no differences between groups for any parameter. The authors concluded that total and cortical wall volume and CSA were accurately assessed using MRI, but width measures were not. However, the authors admitted the most likely reason for the inaccuracy of MRI width measures of the venison bone was the difficulty in defining the corresponding measurement points (ie, MRI and calipers measuring the same area). This was supported by the lack of difference between MRI-derived widths and caliper widths in the homogeneous phantom. Moreover, only the validity of using a single 6 mm thick image was assessed. The validity of using multiple images to assess the entire mid-third of the femur has yet to be conducted.

Reliability of the measurements by MRI was also assessed. Two MRI scans were conducted on thirteen subjects (10 healthy and 3 osteoporotic) approximately one week apart and structural measures were determined for each scan by two different operators. Intraoperator and interoperator variabilities were small for all structural measures with coefficient of variation values ranging between 0.42 % and 3.52 % in the healthy subjects and between 0.68 % and 3.99 % in the subjects with osteoporosis. These numbers are extremely low considering most measurements were taken from a single image 6 mm thick.

The study of Woodhead et al (111) suggests MRI provides an accurate and reliable assessment of the geometric structure of bone. While width measurements from single images may have limited accuracy, multiple images likely provide a better reflection of the entire shaft. This is supported by the lack of statistical difference between estimated and actual volume measurements, which were representative of the entire mid-shaft.

## Bone Deterioration After SCI

### *Effect of SCI on Bone Mineral*

It is clear that there is a rapid decrement in areal bone mineral density (aBMD) and bone mineral content (BMC) and other measures of bone mass associated with unloading of the skeleton. Such changes have been observed following spaceflight (10, 19, 63, 105, 107), extended bedrest (57) and SCI (7, 8, 22, 33, 37, 50, 102, 110), as well as hindlimb unloading in lower mammals (47, 90). In individuals with SCI the loss of bone is particularly striking in the lower limbs (7, 8, 50, 87). Lower limb aBMD and BMC decreases at a rate of 1.5 to 2%/month during the first 4 to 12 months following injury (110). The effect of skeletal unloading appears to have its most profound effect on trabecular bone (8, 22), with rates of loss reported as high as 4 to 5%/month (73, 74, 110). Such a decline is remarkable considering there is only a 3 to 5 % annual reduction in BMD during menopause, a normal physiologic condition associated with marked bone loss (15, 21). Bone mass appears to reach a steady state within 2 years of injury, at which time BMC is 40 to 50% of normal in the proximal tibia and 60-70% of normal in the femoral neck (8).

*Effect of SCI on Trabecular Bone Microarchitecture*

Although numerous studies have reported a rapid loss of aBMD and BMC in the lower limbs following unweighting and SCI, and aBMD provides a strong indication of bone strength and fracture risk (11), there is a significant overlap in those who do and do not experience skeletal fracture. This has led to the current interest in the qualitative aspects of the skeleton and their contribution to skeletal strength. Presently, it is not known if indices of trabecular bone microarchitecture, such as Tb.Th, Tb.N and Tb.Sp, are also diminished following SCI (46). However, a handful of studies conducted on lower mammals provides some insight into the potential response of trabecular bone microarchitecture to skeletal unloading in humans.

In an early study of unloading on trabecular bone microarchitecture of the lumbar vertebrae and proximal femur using radiography, Kazarian and Von Giereke (51) immobilized skeletally mature rhesus monkeys (n = 6) by full-body plaster casts for 60 days. Although statistics were not conducted, the authors reported a reduction in the size and number of trabeculae compared to controls (n = 6). A reduction in the plate size, orientation and porosity of the trabeculae was also noted.

More recent studies reported similar results. Vico et al. (105) studied the effect of 7 days of spaceflight on the architecture of the proximal tibial metaphysis in seven male rats. A dramatically lower BV/TV (55 % and 47 %), Tb.Th (24 % and 20 %), and Tb.N (43 % and 40 %), as determined using bone histomorphometry, were observed in the unloaded rats relative to controls. In a study by Bourrin et al. (10) the response of the proximal tibial metaphysis of 5-week old Wistar rats to 14 days of tail suspension was

examined. The ratio of trabecular bone volume to total volume, Tb.N, Tb.Th and Tb.Sp assessed using bone histomorphotometry were not altered in the primary spongiosa, but lower BV/TV (27.8 %) and Tb.N (23.3 %) were observed in the secondary spongiosa (ie, established skeletal tissue). The changes were accompanied by a reduction in aBMD in the distal, proximal and diaphyseal sections of the femur, with the loss reaching 31 % in the total femur.

Ito et al. (48) studied the effect of neurectomy on trabecular bone microarchitecture on the proximal metaphyses of the tibia in 8-week old Lewis rats. During a 4 week period of immobilization the rats experienced a drastic deterioration of trabecular microarchitecture as evidenced by BV/TV, Tb.Th, T.Sp and Tb.N Z-scores of -2.25, -1.45, 7.00 and -3.31, respectively. An interesting observation was the flake-like appearance in the trabeculae in the rats subjected to neurectomy, as opposed to the diffuse appearance observed in rats ovariectomized.

Together, these studies suggest trabecular bone microarchitecture is lost during extended periods of unloading in lower mammals. While it has been inferred that SCI may alter trabecular bone microarchitecture in the lower limbs of humans (58), there are no published reports.

*Effect of SCI on Bone Structure and Strength*

Our knowledge about the response of bone structure, or macroarchitecture, in the shafts of the lower limbs to SCI is limited to three studies. Lee et al. (58) examined the structure and strength of a limited number of frozen tibias previously amputated from elderly men suffering from peripheral vascular disease (60 to 70 years of age; n = 8).

Four of the tibias were excised from men with SCI and the other four from men who were ambulating. Tibias from the two groups were not statistically different in age, length or weight. Despite the similarity in overall size, the cortical wall was thinner in the SCI tibias than controls with a preferential atrophy in the posterior quadrant of the bone. Although there have been reports that the bone atrophy associated with SCI is most evident at more distal skeletal sites, the degree of deterioration was consistent along the length of the tibia (ie, proximal, middle or distal regions). The flexor modulus of elasticity, as assessed using a four-point bending test, was lower in all quadrants of the bone studied (lateral, medial, anterior and posterior). A region by quadrant effect suggested the reduction in flexor modulus of elasticity in the SCI group was specific to the medial and lateral quadrants of the middle region. Interestingly, there was no statistical difference in polar moment of inertia (J), another indicator of bending stiffness or strength (28). Considering the thinner cortical walls of the tibia in the SCI subjects (up to 49 % in some regions) and the lack of difference in bone size, the latter finding is somewhat surprising.

The lack of difference in J between groups may be related to the extremely small sample size studied (n = 4/group), as well as the complicating effects of age and health status. During the 43 years prior to amputation, the already degenerated tibias may have experienced a lower rate of age-related bone change. Thus, the initial effects of SCI on bone may be less evident in the elderly skeleton. It is also possible that the tibia does not experience as drastic a decline in strength as other long bones in the lower limbs, such as the femur. While this notion corresponds with the lower rise in fracture incidence in the

tibia than the femur following injury (104), it is not consistent with a recent *in vivo* study of the tibia in men with SCI.

de Bruin et al. (23) studied the bone structure, CSMI and bending stiffness of the tibia in 10 men with SCI and a history of lower extremity pathologic fracture after injury, 10 men with SCI without a history of pathologic fracture and 10 ambulating controls. Bone structure and CSMI were measured at 6 regions along the length of the shaft using quantitative computed tomography (QCT). Bending stiffness was assessed using a BSMD-Swing. In the SCI group with a history of fracture, CSMI in the first main axis and the second main axis of the most proximal section of the tibia and the average CSMI of six sections over the length of the tibial shaft were lower than controls (33 % to 41 %; $P < 0.05$). CSMI in the second main axis of the diaphysis in the most distal section of the tibias was also lower than controls (30 %; $P < 0.05$). Moreover, CSA and bending stiffness was reduced by 35 % to 41 %. In the SCI group without a history of fracture, CSMI was not statistically different from controls at any site, but CSA and bending stiffness were 23 to 28 % lower ($P < 0.05$). The observation that the SCI group with previous fracture, but not the non-fracture group, had lower CSMI from controls suggests that geometric properties can help discriminate between those individuals with SCI most at risk for fracture. While the differences in CSMI between the SCI group that did not experience lower limb fracture and controls were not statistically significant, large effect sizes at most sites (Cohen's d range = 0.7 to 1.3) suggest the study was underpowered and that the 17 to 26 % lower CSMI was meaningful. Thus, the findings suggest that individuals with SCI that have yet to experience skeletal fracture in the lower limbs are also at higher risk for fracture of the tibia than normal.

Only one study has assessed structural properties of the femur, the bone that experiences the highest increase in skeletal fracture after SCI (23 fold) (104). In a cross-sectional investigation of 239 men and 7 women 21 to 78 years of age, Kiratli et al. (54) examined the inner and outer diameter of the middle portions of the femur using radiography. From these structural measures polar moment of inertia (J) and polar section modulus (Z; another indicator of bending and torsional strength), were calculated. Despite having thinner cortical walls, neither J nor Z was statistically different between groups.

The authors attributed the lack of impairment in strength to an age-related expansion of the periosteal diameter (ie, outer diameter) and the negligible effects of the inner diameter of the bone in the calculation of J and Z. However, the lack of difference in the outer diameter of the femoral midshaft in the SCI group and controls refutes their contention of an age-related expansion of the periosteum. Although the idea that the outer diameter of the bone is the dominant factor in the calculation of J and Z is probably true, the lack of statistical findings may be attributed to substantial within group variability and/or limitations associated with the radiographic technique in the assessment of bone structure. Assessment of the structure and strength of the entire bone is limited by the two-dimensional image provided by radiography, which does not capture the potentially larger deterioration at the posterior section of the femur. The sensitivity of the technique is also in question; with some studies suggesting that rarefaction of the skeleton cannot be recognized until 30 % of bone mineral is lost (51). Furthermore, it has been suggested that the variability of bone diameter assessment using radiography can be as high as 10 % (40). On the other hand, the reliability of bone structure measurement of

a single slice by more powerful methodologies, such as MRI, is less than 1 % in healthy subjects and less than 4 % in osteoporotic subjects (111). A final limitation of the methodology employed by Kiratli is the small area examined (1 cm). It is possible that a 1 cm region does not reflect the status of the entire femoral shaft.

To summarize, previous studies have assessed the structure of the tibia and femur in adults with SCI. Although all studies report thinner cortical walls and no change in the total diameter of the bones, measures of bending strength are not always statistically different in the SCI groups relative to controls. The maintenance of bone strength following injury reported by some studies does not correspond with the structural deterioration that occurs and the marked rise in fracture incidence in the lower limbs of individuals with SCI (see "Effect on Fracture Incidence" section below). The lack of statistical findings may be limited by the age and health status of the subjects studied, the use of questionable methodologies and the lack of statistical power.

## Potential Mechanisms Underlying Bone Deterioration after SCI

According to Wolff, "the law of bone remodelling is the law to which alterations of the internal architecture clearly observed and following mathematical rules, as well as secondary alterations of the external form of the bones following the same mathematical rules, occur as a consequence of primary changes in the shape and stressing or in the stressing of bones The Law of Bone Remodelling ….." In other words, bone accommodates to the mechanical loads imposed on it and its steady-state should be a reflection of the bones loading history (70). Because mechanical loading is virtually lost

after SCI, uncovering its mechanistic role in the maintenance of bone mass and quality should give insight into the deterioration of bone after injury.

*Mechanisms Underlying the Positive Effect of*

*Mechanical Loading on Bone Mass and Quality*

Several models have been proposed to describe the responsiveness of bone to mechanical loading. These theories are usually predicated on the view that the adaptive response of the skeleton optimizes some objective function, such as the ultimate breaking stress of bone (ie, the ratio of peak stresses to a bones maximum tolerable stress) or strain energy density (ie, the concentration of mechanical energy stored in a material), or simply the strain experienced by a specific bone (ie, change in bone relative to its original length of a bone). Many have embraced the latter as the most likely candidate (70). The notion that bone adapts to maintain the level of strain it experiences is congruent with the extraordinary consistency in the strains experienced by different animals during normal activity (92).

One notable study demonstrating the connection between strain and bone remodeling was by Rubin and Lanyon (93). Using the externally loadable ulna preparation in turkeys these investigators suggested there is a positive relationship between strain magnitude and the change in cross-sectional area of bone. The mid-shaft of one ulna per animal was externally loaded using a servo-hydraulically controlled (Instron) loading machine. The peak loads from the machine were adjusted to create strains at 6 different levels (500, 1000, 1500, 2000, 3000 and 4000 μE (microstrains). Immobolized ulnas were loaded daily for 8 weeks. Bone was lost when strains were

limited to 500 με, maintained at 1000 με and increased at higher strain levels. Despite considerable variability, especially at the higher strain levels, there was a positive relationship between the strain magnitude and the change in CSA of the ulna mid-shaft ($r = 0.83$; $P < 0.05$). In addition to demonstrating a linear relationship between strain magnitude and bone size, this classic study suggested that because the strains imposed on the bone were within the normal physiological limit, strain distribution, in addition to strain magnitude, contributes to the regulation of bone CSA.

Others suggest bone can be maintained without strain. In a recent report by Bergula et al. (5), the effect of increases in interstitial fluid flow on bone was studied in hindlimb suspended and non-suspended rats. In both groups of rats the femoral vein in one limb was ligated for 19 days. While suspension caused a significant decline in femoral aBMD, BMC, proximal width and diaphyseal width ($P < 0.05$), venous ligation increased femoral BMC, length and trabecular density relative to the contralateral limb ($P < 0.05$). Venous ligation had no effect on bone in the non-suspended rat suggesting the effect of normal ambulation and venous ligation stimulate bone accrual via a similar mechanism. An increase in intramedullary fluid pressure was observed in the ligated femur, which was believed to reflect increases in interstitial fluid flow proportional to the pressure drop across the bone.

The cellular mechanisms underlying bone maintenance and gain are also not completely understood. In general it is believed that changes in strain or pressure in bone are transmitted via a mechanical signal. The signal is detected by certain cells that create chemical signals which are believed to modulate bone formation and resorption (28). One type of cell proposed as a detector cell is the osteocyte (25). Osteocytes are mature

osteoblasts embedded within the bone matrix that have the ability to synthesize and resorb matrix. They are housed in a space or lacunae within the matrix and extend filopodial processes through canaliculi. A network of canaliculi extend throughout the bone allowing communication among osteocytes via their filopodial processes and gap junctions. The filopodial process also provide communication between the internal and external surfaces of bone as well as blood vessels that navigate through the matrix (71).

In addition to their ubiquity throughout bone tissue and their ability to communicate with other cells, another feature that makes the osteocyte a strong candidate as a detector cell is its extreme sensitivity to its physical environment (25). More specifically, osteocytes respond to fluid shear stress by producing paracrine factors (56). It is hypothesized that such factors can be transmitted cell to cell to stimulate new bone formation (98).

Turner (98) hypothesizes that if osteocytes are indeed detector cells their connection to mechanical loading may be related to the metabolic needs of the osteocyte. A transcortical pressure gradient in the long bones from the medullary cavity to the periosteum facilitates the perfusion of osteocytes. Mechanical loading likely increases the pressure gradient substantially, leading to a subsequent increase in osteocyte perfusion (98). This notion coupled with the observation that osteocytes within turkey ulnas become hypoxic within 24 hours of unloading, but experience a reversal after a brief out of loading (25), suggests that mechanical loading is necessary for osteocytes to survive.

*Metabolic and Hormonal Consequences of SCI*

Although the mechanisms underlying bone deterioration following SCI are not entirely clear, the metabolic and hormonal responses have been elucidated. Roberts (87) tracked the changes in markers of bone turnover and other hormones involved in the regulation of the skeleton in 14 to 66 year old males (n = 24) and females (n = 6) during the first 24 weeks after injury. There was a significant but small rise in serum total alkaline phosphatase detectable at 3, 4, 6, 8 and 16 weeks after injury. A similar, but not statistically significant, increase was observed in intact osteocalcin, another marker of bone formation. The increase in urinary markers of bone resorption (ie, total and free deoxypyridinoline, pyridinoline and n-telopeptide all relative to creatinine), however, was much more pronounced, reaching levels 10 times greater than normal by 10 -16 weeks after injury. Moreover, these increases were still present at the cessation of the study at 6 months after injury. While use of bone-specific rather than total alkaline phosphatase would be a better indicator of changes in bone formation, the similar response in osteocalcin suggests the markers adequately tracked changes in bone formation. Furthermore, a similar pattern has been reported in men (n = 9) and women (n = 2) exposed to 12 weeks of bed rest (112). Together, these studies suggest there is an uncoupling of bone turnover immediately after SCI with a marked rise in bone resorption outpacing small, if any, increases in bone formation leading to erosion of bone tissue.

In addition to the increase in bone resorption, urinary 24-h calcium excretion tracked the rise in serum ionized calcium but only reached modest levels (< 10 mmol/d). It has been hypothesized that the increase in the serum ionized calcium concentration is detected by the calcium sensor in the parathyroid gland leading to a reduction in the

synthesis and secretion of parathyroid hormone (PTH) (46). This notion corresponds with the concomitant decline in PTH reported in the Roberts study and by others (85).

Since PTH promotes the tubular reabsorption of calcium in the distal convoluted tubule, its decline is not surprising. PTH also affects the conversion of 25-hydroxyvitamin D to 1,25 dihydroxyvitamin D (45), the form of vitamin D that increases the absorption of calcium in the intestines. This is consistent with the lack of change in 25-hydroxyvitamin D but a drop in 1,25-dihydroxyvitamin D below the normal range ($P < 0.05$) in a small sub-sample of quadriplegics ($n = 8$) from the Roberts study.

In summary, there is a decrease in the rate of bone resorption but a small, if any, increase in bone formation. The uncoupling of resorption and formation leads to increased excretion of n-telopeptide, pyridinoline and deoxypyridinoline complexes, as well as calcium, into the urine. Slight increases in the serum ionized calcium concentration that follow appear to be detected by the calcium sensor in the parathyroid glands. Subsequently, the synthesis and secretion of parathyroid hormone PTH is reduced. Low levels of PTH in the serum leads to decreased tubular reabsorption of calcium in the distal convoluted tubules. Since PTH also affects the conversion of 25-hydroxyvitamin D to 1,25 dihydroxyvitamin D (45) it probably contributes to the decreased absorption of calcium in the intestines. This proposed chain of events is a modification of model proposed by Holick (46) explaining the effects of unloading from microgravity or bed rest on calcium metabolism.

Assessment of Skeletal Muscle Using MRI

As with the skeleton, several methods have been developed to assess skeletal muscle *in vivo*. Computed tomography and MRI, without question, provide the most accurate assessment of human contractile tissue. The most convincing evidence is provided by studies of human cadavers. Recently, Mitsiopoulos et al (73) compared skeletal muscle CSA measured by MRI and CT with actual measures obtained using high resolution photography and calibrated rulers. Adipose tissue-free skeletal muscle CSA by MRI CT and the validation method were virtually equivalent as indicated by no mean differences (38.9 ± 23.0 $cm^2$, 39.7 ± 22.8 $cm^2$ and 39.5 ± 23.0 $cm^2$, respectively), very high correlations between MRI and CT measures and the actual measures (r = 0.98 to 0.99) and no difference in slopes from one or differences in intercepts from zero. An interesting observation was that skeletal muscle < 15 $cm^2$ was underestimated by CT, but not by MRI. The remarkable accuracy of MRI was further supported by comparing the volume of two distinctly different-shaped phantoms. Irrespective of phantom shape, there were no differences between MRI-derived volume measures and actual volume.

Mitsiopoulos and colleagues (73) also assessed the reliability of MRI and CT skeletal muscle measurement in the lower limbs. Seven images of the lower limb were collected from six subjects on two different days. The correlation between skeletal muscle from day one and day two were very highly correlated with lower standard errors of estimate (2.9 %). Hence, this study suggests skeletal muscle assessed from MRI provides exceptionally accurate and reliable measures of skeletal muscle.

Skeletal Muscle Deterioration After SCI

Because of the coordinating action between bone and skeletal muscle, studying the effects of SCI on both tissues is logical. While the study of bone structure and quality is still in its infancy stage, the effect of SCI on the mass and quality of skeletal muscle has undergone extensive investigation. As with bone, SCI results in a marked deterioration of lower limb skeletal muscle. Cross-sectional studies have reported lower muscle fiber cross-sectional area (CSA) (41, 72, 79, 88, 91) mitochondrial content (72) and strength (35, 60, 86), as well as an increased fatiguability (43, 60, 86, 89, 94, 97) and % of fast-twitch muscle fibers (41, 72, 80, 91) in chronic SCI patients. Observations that CSA of the gastrocnemius, soleus, quadriceps femoris, hamstring and adductor muscle group decreases 12 to 24 % between 6 and 24 weeks post SCI suggest muscle is lost more rapidly than bone (13). The observed decrement is remarkable considering the fiber CSA's of the SCI patients were already ~60 % of age- and weight-matched able-bodied controls when the study was initiated. The low force that can be evoked by electromyostimulation (EMS), especially in chronic patients, has been attributed to this muscle atrophy (35, 38, 43, 60, 86). Interestingly, force loss during repetitive contractions elicited by EMS is unaltered during the first several months post injury (94), but it is increased one year or more following injury (43, 60, 86, 88, 94, 97).

Despite the wealth of knowledge regarding the decline of skeletal muscle following SCI, it is unclear if the reduction is proportionately greater than other components that comprise the non-fat component of the body. It is often assumed that skeletal muscle represents a certain fraction of the fat-free mass, fat-free soft tissue or adipose tissue-free mass. Based on studies of 24 human cadavers, Clarys et al (18)

reported that the ratio of skeletal muscle to adipose tissue-free mass in the total body was 0.52 in men and 0.50 in women. These findings suggest skeletal muscle represents approximately 50 % of the adipose tissue-free mass. Similar ratios were reported when whole body MRI scans were conducted on healthy men (0.528 ± 0.036) and women (0.473 ± 0.037). However, there is reason to believe that the ratio of skeletal muscle to lean component is lower in men with SCI. In the same study by Wang et al (109), men (n = 11) and women (n = 10) with AIDS were found to have a significantly lower ratio of skeletal muscle to adipose tissue-free mass (0.459 ± 0.033 and 0.433 ± 0.019, respectively).

Such a discrepancy in the skeletal muscle concentration between healthy individuals and individuals with extreme skeletal muscle atrophy, although not an issue when skeletal muscle is assessed using MRI or CT, can be problematic when skeletal muscle is assessed by less direct, although promising, methods such as DXA. The latter technique quantifies bone mineral, fat and FFST mass based on the attenuation properties of these distinctly different tissues. While recent studies support the validity of estimating skeletal muscle from FFST in healthy adults (9, 12, 15), a particularly lower concentration of skeletal muscle in the FFST may yield inaccurate estimates of skeletal muscle by DXA. Moreover, if it is found that skeletal muscle represents a smaller proportion of the FFST than assumed, previous studies that used DXA to estimate skeletal muscle deterioration in the lower limbs of individuals with SCI (96) underestimated the degree of atrophy associated with SCI.

Chapter III

# TRABECULAR BONE MICROARCHITECTURE IS DETERIORATED IN MEN WITH SPINAL CORD INJURY

---

Modlesky, Christopher M., Sharmila Majundar, Anita Narasimhan and Gary A. Dudley. To be submitted to *The Lancet*

Summary

The importance of weight bearing and physical activity for maintenance of bone mineral is recognized, but the mechanisms responsible for modulating trabecular bone microarchitecture have received much less attention. The results of this study comparing able-bodied and clinically complete spinal cord injured young men suggest that long-standing unloading of the skeleton results in marked deterioration of trabecular bone microarchitecture about the knee. Considering the notion that loss of trabecular connectivity is irreversible, these novel findings are of major biological significance. The impaired bone quality is also clinically relevant in that bone mineral per se does not explain fracture risk or incidence.

INDEX WORDS: Trabecular bone, unloading, bone loss, magnetic resonance imaging

Bone mineral content is usually assessed to ascertain risk of fracture because it contributes to breaking strength and can be measured in vivo (2). Mineral, however, is not the sole contributor to skeletal integrity. Significant overlap in measures of bone mineral in those who do and do not fracture has been documented (3). It is reasonable that much of the variance in fracture predictability not accounted for by mineral content is probably related to the microarchitecture of trabecular bone (4). Assessment of human skeletal microarchitecture, however, was not practicable until recently. Fortunately, advances in the application of high resolution computed tomography or nuclear magnetic resonance imaging now make it technologically feasible to conduct heretofore impossible studies of trabecular bone microarchitecture in humans.

Maintenance of skeletal mass is dictated largely by the loads imposed by weight bearing and physical activity. This hypothesis is drawn largely from studies of animals or humans wherein unloading has been shown to evoke the largest decreases in bone mineral for a given duration compared to other interventions (6). It also appears that loading is critical for maintenance of skeletal microarchitecture based on the results of the few studies that have been conducted in lower mammals (6). Considering that clinically complete spinal cord injury (SCI) results in loss of motor function below the level of injury and unparalleled deterioration of affected bone mineral mass, this condition represents a unique model to study the significance of weight bearing and skeletal muscle use upon bone microarchitecture in humans. Accordingly, we assessed trabecular bone microarchitecture in eight young men with complete SCI (C6 - L1; n = 8; 34 ± 10 y; 178 ± 11 cm; 76 ± 22 kg) 2.3 to 20.1 years post injury (mean 8.7 ± 7.5 y) and 8 able bodied males (33 ± 10 y; 176 ± 9 cm; 78 ± 16 kg) to address this issue. None of

the subjects had a history of chronic medication use and all denied lower limb fracture. The study was approved by the Institutional Review Board at the University of Georgia and at the Shepherd Center and written consent was given by each subject before testing.

Sixty high resolution axial images (reconstructed spatial resolution = 195 x 195 by 1000 $\mu^3$) of the distal femur and of the proximal tibia were collected on a GE 1.5 T magnetic resonance imager using a 3D fast gradient echo sequence with a partial echo acquisition (echo time = 4.5 ms; repetition time = 30 ms; 40° flip angle; 15.6 kHz bandwidth), a 10 cm field of view and an imaging matrix of 512 x 384. Measures of trabecular bone microarchitecture, such as apparent trabecular bone volume to total volume (appBV/TV), trabecular number (appTb.N, $mm^{-1}$), trabecular thickness (appTb.Th, mm), and trabecular separation (appTb.Sp, mm), were determined using previously described methods (1). In short, a 3-D low-pass filter-based correction was applied to images to eliminate potential inhomogeniety caused by the surface coils. Regions of interest were drawn manually over approximately 30 images of each bone. Images were thresholded using a dual reference limit that assumes a biphasic model and were segmented into bone and marrow phases. The segmented binary images were used to calculate appBV/TV, appTb.N, appTb.Th and appTb.Sp.

The distal femur of the SCI group had fewer trabeculae (appTb.N, 21 %) that were thinner (appTb.Th, 7 %) and further apart (appTb.Sp, 43 %) than in the able-bodied group, resulting in less bone per unit volume after injury (appBV/TV, 26 %) ($p < 0.05$; Table 3.1). Differences were also noted for the proximal tibia appTb.N, (19 % lower), appTb.Sp (32 % higher) and appBV/TV (18 % lower) ($p < 0.05$; Table 3.1). This marked deterioration is visualized in a representative high-resolution image (Figure 3.1). In this

T1, axial image of the femur, less trabecular bone, "black lines," and more marrow (white) are clearly evident after injury. The nature of retrogression of trabecular bone also was different in the tibia than in the femur. The volume and number of trabeculae decreased to a greater extent as distance from the joint line increased distally in the tibia in SCI than in able-body subjects while the opposite was the case for spacing. Differences in microarchitecture between groups along the length of the femur, in contrast, were consistent. Why the apparent divergent responses between bones is not clear, but they do suggest that deterioration increased more distally in the leg than thigh, this response keeping with previous changes in mineral content and fluid redistribution with unloading.

These findings suggest that the deterioration associated with extreme unloading is not limited to bone mass, but also includes trabecular bone microarchitecture. Prior studies have observed impaired microarchitecture in vertebral fracture patients versus controls, however, the subjects were typically > 50 years of age and the reason for the reduced bone quality was not determined (4). In the present study, the subjects were young (34 ± 10 y) and the reason for the bone deterioration is apparent. Considering there is a marked increase in fracture after SCI, these findings are of clinical significance. Because deteriorated trabeculae are thought to lack the capacity to regenerate (5), the findings are also of biological significance.

This study suggests the effect of ambulation and skeletal muscle activity in the maintenance of skeletal tissue quality is powerful. Whether individuals exposed to other unloading conditions, such as extended bedrest or spaceflight also exhibit substantially impaired trabecular infrastructure of weight-bearing bones has yet to be determined.

References

1. Beuf, O., S. Ghosh, D. C. Newitt, T. M. Link, L. Steinbach, M. Ries, N. Lane, and S. Majumdar. Magnetic resonance imaging of normal and osteoarthritic trabecular bone structure in the human knee. Arthritis Rheum 46: 385-93., 2002.

2. Bouxsein, M. L., B. S. Coan, and S. C. Lee. Prediction of the strength of the elderly proximal femur by bone mineral density and quantitative ultrasound measurements of the heel and tibia. Bone 25: 49-54, 1999.

3. Cummings, S. R. Are patients with hip fractures more osteoporotic? Review of the evidence. Am J Med 78: 487-94, 1985.

4. Legrand, E., D. Chappard, C. Pascaretti, M. Duquenne, S. Krebs, V. Rohmer, M. F. Basle, and M. Audran. Trabecular bone microarchitecture, bone mineral density, and vertebral fractures in male osteoporosis. J Bone Miner Res 15: 13-9, 2000.

5. Parfitt, A. M. Trabecular bone architecture in the pathogenesis and prevention of fracture. Am J Med 82: 68-72, 1987.

6. Vico, L., D. Chappard, S. Palle, A. V. Bakulin, V. E. Novikov, and C. Alexandre. Trabecular bone remodeling after seven days of weightlessness exposure (BIOCOSMOS 1667). Am J Physiol 255:R243-7, 1988

Table 3.1. Measures of trabecular bone microarchitecture in men with spinal cord injury (SCI) and controls

| | SCI (n = 8) | Controls (n = 8) |
|---|---|---|
| Femur | | |
| appBV/TV | 0.231 ± 0.029* | 0.314 ± 0.029 |
| appTb.N ($mm^{-1}$) | 1.087 ± 0.113* | 1.371 ± 0.097 |
| appTb.Th (mm) | 0.212 ± 0.012* | 0.228 ± 0.013 |
| appTb.Sp (mm) | 0.724 ± 0.105* | 0.506 ± 0.060 |
| Tibia | | |
| appBV/TV | 0.234 ± 0.030* | 0.284 ± 0.035 |
| appTb.N ($mm^{-1}$) | 1.103 ± 0.109* | 1.368 ± 0.203 |
| appTb.Th (mm) | 0.219 ± 0.049 | 0.209 ± 0.008 |
| appTb.Sp (mm) | 0.711 ± 0.088* | 0.539 ± 0.095 |

Values are means ± SD

*Different from controls ($P < 0.05$)

appBV/TV = apparent bone volume/total volume

appTb.N = apparent trabecular bone number

appTb.Th = apparent trabecular bone thickness

appTb.Sp = apparent trabecular bone separation

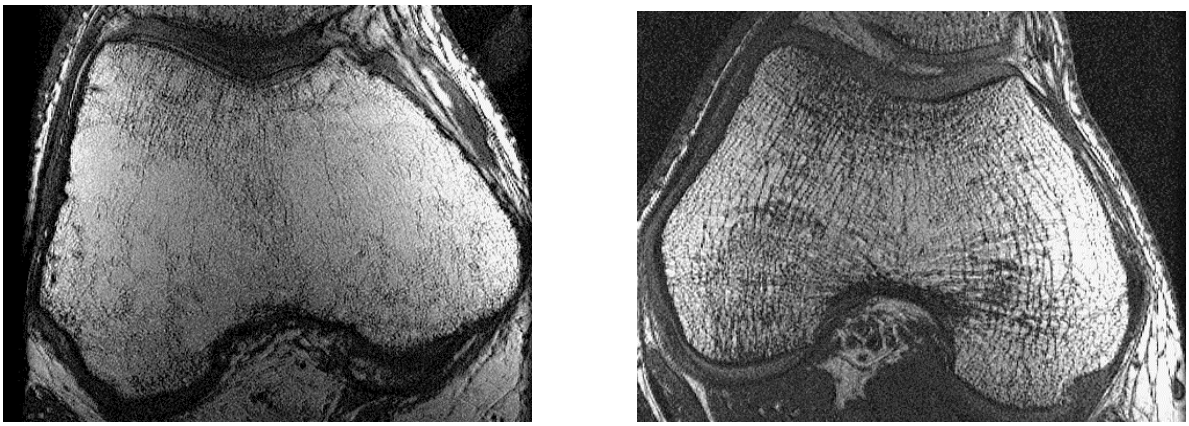

Figure 3.1. High-resolution images of the distal femur bone of a spinal cord injured subject on the left and an able-bodied control on the right. Notice the fewer black lines (bone) and more white (marrow) in the image of the spinal cord injured subject.

Chapter IV

# THE EFFECTS OF UNLOADING ON GEOMETRIC STRUCTURE AND STRENGTH OF BONE IN MEN WITH COMPLETE SPINAL CORD INJURY

---

Modlesky, Christopher M., Jill Slade, Christopher S. Bickel and Gary A. Dudley

To be submitted to *Bone*

Abstract

It is clear that bone mineral mass is markedly reduced in the lower limbs following extreme skeletal unloading, such as occurs after spinal cord injury (SCI). However, the degree of deterioration in structure and strength has received limited attention. The purpose of the present study was to assess bone structure and strength in the mid-femur of men with complete SCI (n = 7) 2.3 to 20.0 years (mean ± SD; 7.7 ± 6.0 years) post injury and healthy able-bodied controls (CON; n = 8). Axial images of the femur were collected on a GE 1.5 T magnetic resonance imager using a T1 weighted sequence. There were no differences in age (34.1 ± 9.3 y vs 32.5 ± 8.7 y), height (179.2 ± 8.5 cm vs 177.4 ± 7.3 cm), or weight (79.6 ± 21.5 kg vs 78.7 ± 20.7 kg) between SCI and CON, respectively. While the volume of the total mid-femur was not different in the two groups and the width in the mediolateral and anteroposterior directions was only slightly smaller in SCI (3 and 6%; $P < 0.05$), the composition of the bones was much different. Volume and width of the medullary cavity were 54.1 % and 21-23 % larger in SCI. Although not statistically significant ($P = 0.059$), a large effect size (partial eta squared = 0.25) indicated a larger volume of the endosteum in SCI than CON (44 %). In contrast, cortical volume was 23 % lower and the lateral, medial, anterior and posterior aspects of the cortical wall were 22 to 39 % lower in SCI. The cortical wall was particularly thin and the endosteum particularly thick in the posterior section in the SCI group ($P < 0.05$). The structural compromise was accompanied by lower cross-sectional moment of inertia, polar section modulus and bone strength index (15 to 35 %). While the thickness of the cortical wall and indices of bone strength were lower at the most distal portion than the most proximal portion of the mid-femur ($P < 0.05$), the degree of difference was similar

in SCI and CON ($P > 0.05$). The findings suggest that after SCI the mid-femur deteriorates from the inside out with the greatest degree of deterioration in the posterior aspect of the bone. The result is a subsequent decrease in bone strength, consistent with the remarkably high incidence of fracture in the femur after injury.

INDEX WORDS: Bone geometry, cross-sectional moment of inertia, polar moment of inertia, polar section modulus, bone strength index, magnetic resonance imaging

## Introduction

The integrity of the skeleton is dictated by its mineral mass and structure. These bone parameters are closely tied to mechanical loading. More specifically, the strain rate, magnitude and distribution associated with weight-bearing and normal physical function appear to drive the mineralization and geometric structure of the skeleton (14, 15). The importance of ambulation and general physical movement in the maintenance of skeletal mass has been documented in lower mammals and humans (8). For instance, extended bed rest (12) and spinal cord injury (SCI) (2) are associated with a marked decline in bone mineral content (BMC). Sites most affected by unloading are weight-bearing bones such as the femur and tibia, with the greatest loss of BMC occurring at the most distal skeletal sites (12).

Measures of bone mineral mass are typically used to assess fracture risk. Although BMC and areal bone mineral density (aBMD) from dual-energy X-ray absorptiometry (DXA) correlate strongly with breaking strength and bone fracture (3), these mineral measures provide an incomplete picture of bone competence. The study of the structural aspects of bone should provide a more thorough understanding of its biology, strength and dependence on basic loading patterns (6). Studies of adult dogs exposed to unloading conditions suggest there is a thinning of the cortical walls, however, the surface of the bone deterioration is dependent on the age of the skeleton. For instance, in young adult dogs unloading leads to a reduction in total bone width due to erosion of the periosteal surface of bone (18). In contrast, the decline of bone in older dogs is primarily due to erosion on the endocortical surface, leading to an expansion of the medullary cavity (10). The structural deterioration of bone in lower mammals is

associated with a reduction in cross-sectional moment of inertia (CSMI) and ultimate failure load (7).

The effect of unloading on bone structure and strength is poorly studied in humans. Moreover, only one study focused on the femur (11), the bone that experiences the greatest increase in fracture risk as evidenced by the 23-fold increase in fracture after SCI (19). The report of impaired bone structure in SCI subjects relative to controls coupled with the fracture pattern associated with SCI are, however, incongruent with the report of no reduction in polar moment of inertia (J), a measure of resistance to bending and torsional loads. The peculiar findings may be related to the use of radiography to estimate bone structure and subsequently J. The two-dimensional images produced by radiography coupled with its relatively high variability (9) may limit its ability to assess bone structure and strength.

Magnetic resonance imaging (MRI), on the other hand, allows for unparalleled 3-dimensional visualization of the human body and provides accurate and reliable quantification of bone structural parameters, such as bone CSA and volume (20). Subsequently, MRI-derived structural measures likely yield better and more sensitive estimates of J and other indicators of bone's breaking strength. Furthermore, MRI-derived structural measures of bone can be combined with BMC from DXA to determine volumetric BMD (vBMD), a better indicator of fracture risk than the widely used aBMD, and bone strength index (BSI), possibly the single best in vivo measure of long-bone bending strength (6). The purpose of the present study was to compare the bone structure and strength of the mid-femur in men with complete SCI, an extreme unloading condition, with able-bodied controls using MRI. We hypothesized that the volume and

width of the total mid-femur would not be different in the two groups, but that these structural measures would be higher for the medullary cavity and the endosteum, and lower for cortical bone resulting in compromised bone strength in men with SCI.

## Methods

### *Subjects*

Men with complete SCI at the C6-L1 level and at least 2 years post injury (n = 8) were recruited for the study from the Shepherd Center, Atlanta, GA. Healthy men of similar age, height and weight to SCI were recruited from the general population (CON; n = 8). Exclusion criteria for the 2 groups were a history of chronic medication use of any kind and prior fracture of the femur or tibia. The study was approved by the University's Institutional Review Board and written consent was given before testing.

### *Bone Structure*

Approximately 25 axial T1 weighted images (1 cm thick separated by 0.5 cm) of the femur were collected on a GE 1.5 Tesla MRI using a whole body coil (TR/TE 500/14 20-24 FOV, 1 NEX, 256 x 256 matrix). Images were downloaded to CD and those representing the mid-femur (~10 images/subject) were analyzed on a PC using a modification of the X-Vessel software program (developed by Ronald Meyer, PhD). Pixels were separated into 3 different categories based on signal intensity and anatomical location. In general, pixels with low, intermediate and high signal intensity were defined as cortical bone, the endosteum and marrow (ie, medullary cavity), respectively. Pixels from each region (cortical, endosteal and medullary cavity) were summed to determine

the region's CSA. The CSA of the total bone was determined by summing the CSA's from each region. Volume of the total mid-femur and its specific regions (cortical, CV; endosteal, EV; medullary, MV) were quantified by multiplying each slice by 1.5 to account for the 1 cm thickness of each image and the 0.5 cm gap between slices. After locating the center of the bone, width of the total bone (TW) and the medullary cavity (MW) in the mediolateral direction and the anteroposterior direction and the lateral, medial, anterior and posterior aspects of the cortical (CW) and endosteal (EW) regions were determined by counting the number of pixels and adjusting for pixel size. To ensure consistency, all images were analyzed by one investigator.

*Dual-energy X-ray Absorptiometry*

Total body scans conducted using DXA (Delphi A; Hologic, Inc) were used to assess the bone area, BMC and aBMD of the mid-femur of a single leg and both arms. These scans were also used to measure femoral length, from which the mid-femur was determined. The correlation between femoral length measured by DXA and MRI was excellent ($r = 0.99$; unpublished observations). A calibration step wedge, consisting of thermoplastic resin (68% fat) and thermoplastic resin-aluminum (-10% fat) steps calibrated against stearic acid (100% fat) and water (8.6% fat; Hologic, Inc.) was scanned prior to testing to calibrate fat mass and fat-free soft tissue mass. Quality control was checked before each test session by scanning a lumbar spine phantom consisting of calcium hydroxyapatite embedded in a cube of thermoplastic resin (model DPA/QDR-1; Hologic x-caliber anthropometric spine phantom). The coefficient of variation of the

phantom aBMD during the 3-month period of testing was 0.36%. To ensure consistency, one trained technician performed and analyzed all scans.

*Bone Strength*

Strength measures of the mid-femur were estimated using the bone structure parameters described above and BMC. Specifically, CSMI, J and section polar modulus (Z) were estimated in the mediolateral plane and in the anteroposterior plane of each image of the mid-femur (~10 slices) using the equations below (11, 17)]:

$$CSMI = \pi/4\ (TW^4 - (MW^4 + EW^4)$$

$$J = 2\pi\ (TW^4 - (MW^4 + EW^4))/64$$

$$Z = J/(0.5*TW)$$

Volumetric BMD (vBMD) of the mid-femur was determined the following equation:

$$vBMD = BMC/TV$$

Cortical vBMD of the mid-femur was determined by dividing BMC by CV.

$$\text{cortical vBMD} = BMC/CV$$

Bone strength index (BSI), an excellent indicator of the ultimate failure load of bone, was determined using the following equation (6):

$$BSI = \text{cortical vBMD} \times CSMI$$

*Statistics*

Independent t-tests were used to determine if SCI and CON differed in anthropometrics and TV, MV, CV and EV in the mid-femur. A mixed model two-way ANOVA was used to determine if SCI and CON differed in TW, CW, MW, EW, CSMI, J, Z or BSI in the mediolateral and anteroposterior directions (group by direction), and width (group by width) in the lateral, medial, anterior and posterior regions of the cortical wall and endosteum. Moreover, it was used to determine if there were site effects (ie, medial, lateral, anterior and posterior) or group by site effects. A mixed model (group by distance) two-way ANOVA was also used to determine if measures of bone structure and strength were more deteriorated in the distal vs proximal portion of the mid-femur in SCI vs controls (group by distance effect). Post hoc tests were conducted and the Bonferroni method employed.

The magnitude of effects was assessed using partial eta squared ($\eta^2$). Partial eta squared values of 0.01, 0.06 and 0.14 indicate small, medium and large effects. All data were screened for outliers. One SCI subject was identified as a consistent outlier for several dependent factors (> 3 SD from mean) and was removed from the analysis. Subsequently, all analyses include 7 SCI and 8 control subjects.

Results

Age, height, weight and femoral length, respectively, in SCI (34.1 ± 9.3 y, 179.2 ± 8.5 cm, 79.6 ± 21.5 kg, 47.5 ± 2.8 cm) were not different from controls (32.5 ± 8.7 y; 177.4 ± 7.3 cm; 78.7 ± 20.7 kg, 46.8 ± 2.3 cm). The average time since injury in SCI was 7.7 ± 6.0 y (range = 2.3 to 20.0 y). Measures of bone volume are listed in Table 4.1. Total bone volume was not different between groups, but MV was 54.1 % higher and CV 22.7 % lower in SCI ($\eta^2$ =0.529 and 0.427, respectively, $P < 0.05$). Although not statistically significant, a large effect size ($\eta^2 = 0.249$, $P = 0.059$) indicated a larger EV as well (44.0 %).

Total and regional bone width measures are reported in Table 4.2. A moderate-to-large effect size ($\eta^2 = 0.132$, $P = 0.057$) indicated a slightly smaller TW in SCI than CON (3 to 6 %). There was also a significant plane effect for TW ($\eta^2 = 0.305$, $P < 0.05$), with greater anteroposterior TW than mediolateral TW in SCI (6.9 %) and CON (10.1 %). A significant group effect ($\eta^2 = 0.436$, $P < 0.05$) indicated greater mediolateral MW (23 %) and anteroposterior MW (20 %) in SCI than CON and a significant plane effect ($\eta^2 = 0.259$, $P < 0.05$) indicated greater anteroposterior MW than mediolateral MW in SCI (12.6 %) and CON (15.4 %).

A significant group by site interaction was observed for CW ($\eta^2 = 0.266$, $P < 0.05$). While all sites of the cortical wall (ie, lateral, medial, anterior and posterior) were thinner in SCI than CON (22 to 39%; $\eta^2 = 0.140$ to 0.201, $P < 0.05$), the pattern of site differences was dissimilar in the two groups. In CON, the posterior and lateral regions of the cortical wall were both wider than the medial and anterior regions; whereas, in SCI, only the lateral region was wider.

There were no group differences in EW at any site, however, there was a significant group by site interaction ($\eta^2 = 0.145$, $P < 0.05$). Post hoc analyses revealed a wider EW in the posterior region of the shaft than the lateral ($\eta^2 = 0.579$, $P < 0.05$), medial ($\eta^2 = 0.694$, $P < 0.05$) and anterior ($\eta^2 = 0.611$, $P < 0.05$) regions in SCI, whereas, no differences existed in CON.

Bone area, BMC, aBMD and vBMD of the mid-femur and bone area, BMC and aBMD of the arms are reported in Table 4.3. There were no differences in bone area or cortical vBMD in the mid-femur, but BMC, aBMD and vBMD were 19.3 %, 21.9 % and 16.2% lower in SCI than CON ($\eta^2 = 0.379$, 0.709 and 0.520, respectively, $P < 0.05$). Despite the large differences in the bone mineral measures in the mid-femur, there were no significant group differences in bone area ($\eta^2 = 0.009$, $P = 0.738$), BMC ($\eta^2 = 0.080$, $P = 0.307$) or aBMD ($\eta^2 = 0.105$, $P = 0.239$) in the arms, suggesting that other than the lower limbs, the size and degree of mineralization in the bones of the two groups was similar.

Measures of bone strength are listed in 4. 4. There were significant group ($\eta^2 = 0.263$, $P < 0.05$) and plane ($\eta^2 = 0.176$, $P < 0.05$) effects for CSMI, with mediolateral CSMI and anteroposterior CSMI being 18 % and 20 % lower in SCI than CON and CSMI estimated from mediolateral width measures being 29 % and 31 % less than CSMI estimated from anteroposterior width measures in SCI and CON. respectively. Identical results were found for J. There were also significant group ($\eta^2 = 0.405$, $P < 0.05$) and plane ($\eta^2 = 0.227$, $P < 0.05$) effects for Z. Z from mediolateral and anteroposterior width measures was 16 % and 20 % lower in SCI than CON, whereas mediolateral Z was 20 % and 24 % less than anteroposterior Z in SCI and CON, respectively. There was a

significant group effect for BSI ($\eta^2 = 0.280$, $P < 0.05$), with mediolateral BSI and anteroposterior BSI 22.7 % and 35.3 % lower in SCI, respectively. Moreover, there was a significant plane effect for BSI ($\eta^2 = 0.208$, $P < 0.05$) with mediolateral BSI 17.2 % and 30.7 % lower than anteroposterior BSI in SCI and CON, respectively.

When the proximal and distal portions of the mid-femur were examined, there were no distance or group by distance effects ($\eta^2 \leq 0.025$, $P > 0.05$) for TV, mediolateral TW or anteroposterior TW. There were, however, distance effects for MV ($\eta^2 = 0.521$, $P < 0.05$) mediolateral MW ($\eta^2 = 0.470$, $P < 0.05$) and anteroposterior MW ($\eta^2 = 0.442$, $P < 0.05$). Post hoc analyses indicated greater MV, mediolateral MW and anteroposterior MW at the most proximal vs the most distal portion of the mid-femur in SCI and CON.

There were distance effects for CV ($\eta^2 = 0.476$, $P < 0.05$) and CW in the lateral ($\eta^2 = 0.422$, $P < 0.05$), medial ($\eta^2 = 0.381$, $P < 0.05$) and anterior ($\eta^2 = 0.494$, $P < 0.05$) portions of the cortical wall, with lower CV and CW distally than proximally. There was no significant distance effect for CW of the posterior portion of the wall ($\eta^2 = 0.091$, $P = 0.119$). The lack of group by distance interactions at any site suggests the degree of deterioration in the cortical wall of SCI was equivalent in the most proximal and most distal portions of the mid-femur.

There was a significant group by distance interaction for posterior EW ($\eta^2 = 0.455$, $P < 0.05$). While EW in SCI was greater than CON at the proximal and distal ends, the difference was greater at the proximal end. The discrepancy was due to EW in SCI being twice as great at the proximal end, whereas the EW at the two ends in CON were not different.

There were no distance or group by distance effects for bone area, but SCI and CON had 26.4 % and 26.2 % lower BMC ($\eta^2 = 0.438$, $P < 0.05$) and 34.4 % and 19.3 % lower aBMD ($\eta^2 = 0.694$, $P < 0.05$) distally than proximally.

There were no significant distance or group by distance effects for any strength measure.

## Discussion

The purpose of the present study was to examine geometric structure and calculated strength of the mid-femur in men with complete SCI and able-bodied controls using MRI. A major finding was a substantial difference in the structural composition and strength of the mid-femur despite the lack of difference in TV and a limited difference in TW between the two groups. Specifically, MV was more than 50% larger, MW 20-23 % larger and EV 44 % higher in the SCI group. Conversely, CV was 23% lower and CW 22 to 39% thinner in the SCI subjects. A lower CSMI, J and BSI accompanied these structural impairments.

To our knowledge, this is the first study to use MRI to assess geometric structure of bone in the lower limbs of individuals exposed to extreme unloading. It is also the first study to assess the structure of the femur using a technique with 3D imaging capability. The observation that the cortical walls were 22 to 39 % thinner is consistent with previous studies of the femur and tibia. Although the finding that CSMI and J were reduced in the SCI group is not consistent with all previous studies, it is congruent with the structural impairment observed and the 23-fold increase in fracture incidence in the femur after SCI (19).

The disagreement with two (11, 13) of the three (5, 11, 13) prior studies conducted in individuals with SCI may be attributed to the methodology employed, the specific bones and the size of the area assessed, as well as the age and health of the bones when tested. In a study of men and women with long-standing SCI (11), the observation that J was not lower in the mid-femur despite thinner cortical walls may be explained by the relatively high variability and the two-dimensional nature of the technology employed (ie, radiography). The error of structural measures from radiography can be as high as 10 % (9). Whereas, the error of bone structure measurement by MRI for a single slice is less than 4 % in healthy and osteoporotic subjects (20). Moreover, the radiographic assessment of bone structure in the mediolateral plane did not capture the preferential atrophy of the posterior portion of the mid-femur. An additional factor that may have contributed to the discrepant findings is the limited area measured. In the present study, the area measured was ~ 15.5 cm vs the 1 cm area studied by Kiratli et al. (11). It is possible that radiography-derived width measures of a small area of the femur are simply not sensitive enough to detect differences in bone strength.

In a study of a limited number of tibias previously amputated from elderly men suffering from peripheral vascular disease (n = 4), Lee et al. (13) reported no difference in J from control tibias, which were from able-bodied men also suffering from peripheral disease. It is possible that the tibial shaft exhibits a less pronounced or different response to unloading than the femur resulting in less of a compromise in bone strength, which is supported by the lower relative increase in fracture in the leg than the thigh (5.2 vs 23.4 %) (19). Moreover, the effects of age and health status may have complicated the effects of SCI on bone strength. During the 43 years prior to amputation, the already-

degenerated tibias may have experienced a lower rate of age-related bone change. Thus, the initial effects of SCI on bone may be less evident in the elderly skeleton. Contrary to the findings by Lee et al. (13), de Bruin et al. (5) reported lower bending stiffness and reduced cross-sectional area in the mid-tibia of younger men with SCI.

To our knowledge, this is the first study to assess BSI in individuals with SCI. BSI, a strength measure that reflects the combined influences of the mineral and biomechanical properties of bone, has been shown to correlate better with fracture load than aBMD, cortical vBMD or CSMI (6). Our finding of a lower BSI suggests the overall strength of the mid-femur is impaired following SCI. The lack of difference in cortical vBMD between groups suggests the lower BSI was attributed to reduced biomechanical strength (ie, CSMI).

The preferential atrophy of the posterior section of the mid-femur, as demonstrated by the particularly thin cortical wall and thick endosteum was an interesting observation. Although previously demonstrated in excised tibias, no studies have reported such a phenomenon in vivo or specifically in the femur of young healthy men with SCI. One explanation for the selective deterioration is that the posterior aspect of the mid-femur is the attachment site for a number of muscles, including the vastus lateralis, a leg extensor muscle that experiences a 66% to 75% reduction in fiber CSA within six months of injury (4). The interplay between muscle and bone during ambulation and other physical activity contributes to the development of condyles and crests, geometric features that contribute to the strength of the bone. It is possible that because the linea aspera, a crest at the posterior surface of the femur, is no longer

receiving mechanical stimuli from the vastus lateralis and a variety of other muscles, it retracts during extended periods of disuse.

While the loss of muscular interaction with bone at specific sites likely contributes to some of the deterioration in bone mineral mass and structure, there are probably other contributing factors. It is postulated that in the vertical position a fluid pressure gradient from the top of the body to the bottom caused by gravity provides a stimulus for skeletal maintenance through increased fluid pressure in the medullary cavity (16). The increase in intramedullary fluid pressure is hypothesized to increase transcortical fluid flow resulting in the creation of fluid shear stresses and a stimulus for bone maintenance (16). Such an idea is supported by a recent report in which the inhibition of bone apposition in the femur of hindlimb suspended rats was blunted by ligation of the femoral vein and the subsequent increase in intramedullary cavity pressure (1). Studies are needed to discern between the site-specific effects of muscle-bone interplay and the effects of vertical positioning on skeletal maintenance.

Another novel feature of the present study was the comparison of the structural deterioration in the proximal vs the distal portions of the mid-femur. Previous studies have suggested a preferential loss of bone mineral in the more distal aspects of the skeleton of individuals exposed to extended unloading (12). However, until now, there were no in vivo studies of bone structure or studies of the mid-femur. The observation that the proximal and distal portions of the mid-femur were equally compromised is consistent with findings in the proximal and distal aspects of excised tibias (13). Together, these studies suggest that the highly-cortical shafts of long bones are not affected by the preferential-atrophy phenomenon.

To summarize, the mid-femur of young men with complete and long-standing SCI is normal in size but has thin cortical walls, especially in the posterior region, and an expanded endosteum and medullary cavity.

Bone strength calculations suggest these structural alterations are associated with decreased resistance to bending and torsional loads. Because of the remarkable increase in fracture in the femur after SCI, identifying strategies to combat the loss of bone mineral and structure are sorely needed.

References

1. Bergula, A. P., W. Huang, and J. A. Frangos. Femoral vein ligation increases bone mass in the hindlimb suspended rat. *Bone* 24: 171-7., 1999.

2. Biering-Sorensen, F., H. H. Bohr, and O. P. Schaadt. Longitudinal study of bone mineral content in the lumbar spine, the forearm and the lower extremities after spinal cord injury. *Eur J Clin Invest* 20: 330-5, 1990.

3. Bouxsein, M. L., B. S. Coan, and S. C. Lee. Prediction of the strength of the elderly proximal femur by bone mineral density and quantitative ultrasound measurements of the heel and tibia. *Bone* 25: 49-54., 1999.

4. Castro, M. J., D. F. Apple, Jr., R. S. Staron, G. E. Campos, and G. A. Dudley. Influence of complete spinal cord injury on skeletal muscle within 6 mo of injury. *J Appl Physiol* 86: 350-8, 1999.

5. de Bruin, E. D., R. Herzog, R. H. Rozendal, D. Michel, and E. Stussi. Estimation of geometric properties of cortical bone in spinal cord injury. *Arch Phys Med Rehabil* 81: 150-6., 2000.

6. Ferretti, J. L., R. F. Capozza, and J. R. Zanchetta. Mechanical validation of a tomographic (pQCT) index for noninvasive estimation of rat femur bending strength. *Bone* 18: 97-102., 1996.

7. Garber, M. A., D. L. McDowell, and W. C. Hutton. Bone loss during simulated weightlessness: a biomechanical and mineralization study in the rat model. *Aviat Space Environ Med* 71: 586-92., 2000.

8. Giangregorio, L., and C. C. Blimkie. Skeletal adaptations to alterations in weight-bearing activity: a comparison of models of disuse osteoporosis. *Sports Med* 32: 459-76, 2002.

9. Greenfield, M. A. Current status of physical measurements of the skeleton. *Med Phys* 19: 1349-57., 1992.

10. Jaworski, Z. F., M. Liskova-Kiar, and H. K. Uhthoff. Effect of long-term immobilisation on the pattern of bone loss in older dogs. *J Bone Joint Surg Br* 62-B: 104-10., 1980.

11. Kiratli, B. J., A. E. Smith, T. Nauenberg, C. F. Kallfelz, and I. Perkash. Bone mineral and geometric changes through the femur with immobilization due to spinal cord injury. *J Rehabil Res Dev* 37: 225-33., 2000.

12. Leblanc, A. D., V. S. Schneider, H. J. Evans, D. A. Engelbretson, and J. M. Krebs. Bone mineral loss and recovery after 17 weeks of bed rest. *J Bone Miner Res* 5: 843-50, 1990.

13. Lee, T. Q., T. A. Shapiro, and D. M. Bell. Biomechanical properties of human tibias in long-term spinal cord injury. *J Rehabil Res Dev* 34: 295-302, 1997.

14. O'Connor, J. A., and L. E. Lanyon. The influence of strain rate on adaptive bone remodelling. *Journal of Biomechanics* 15: 767-781, 1982.

15. Rubin, C. T., and L. E. Lanyon. Regulation of bone mass by mechanical strain magnitude. *Calcif Tissue Int* 37: 411-417, 1985.

16. Turner, C. H. Site-specific skeletal effects of exercise: importance of interstitial fluid pressure [comment]. *Bone* 24: 161-2, 1999.

17. Turner, C. H., and D. B. Burr. Experimantal techniques for bone mechanics. In: *Bone Mechanics Handbook*, edited by S. C. Cowen. Boca Raton: CRC Press, 2001, p. 1-35.

18. Uhthoff, H. K., and Z. F. Jaworski. Bone loss in response to long-term immobilisation. *J Bone Joint Surg Br* 60-B: 420-9., 1978.

19. Vestergaard, P., K. Krogh, L. Rejnmark, and L. Mosekilde. Fracture rates and risk factors for fractures in patients with spinal cord injury. *Spinal Cord* 36: 790-6, 1998.

20. Woodhead, H. J., A. F. Kemp, C. J. R. Blimkie, J. N. Briody, C. S. Duncan, M. Thompson, A. Lam, R. Howman-Giles, and C. T. Cowell. Measurement of midfemoral shaft geometry: repeatability and accuracy using magnetic resonance imaging and dual-energy X-ray absorptiometry. *J Bone Miner Res* 16: 2251-9., 2001.

Table 4.1. Total and regional bone volume in men with spinal cord injury (SCI) vs controls (CON)

| | SCI (n = 7) | CON (n = 8) |
|---|---|---|
| Total volume ($cm^3$) | 97.3 ± 19.5 | 97.0 ± 12.1 |
| Cortical volume ($cm^3$) | 51.6 ± 9.9[1] | 66.8 ± 9.6 |
| Endosteal volume ($cm^3$) | 12.1 ± 4.7[2] | 8.4 ± 1.7 |
| Medullary cavity volume ($cm^3$) | 33.6 ± 6.3[1] | 21.8 ± 5.7 |

[1]Different from CON, $P < 0.05$

[2]Different from CON, $P = 0.059$, $\eta^2 = 0.249$

Table 4.2 Total and regional bone width in men with spinal cord injury (SCI) vs controls (CON)

| | SCI (n = 7) | CON (n = 8) | Effect |
|---|---|---|---|
| Total bone width (mm) | | | group[1], plane[3] |
| Mediolateral | 27.7 ± 1.4 | 28.6 ± 2.3 | |
| Anteroposterior | 29.6 ± 2.0 | 31.5 ± 1.9 | |
| Medullary cavity width (mm) | | | group[2], plane[3] |
| Mediolateral | 15.71 ± 1.27 | 12.77 ± 2.54 | |
| Anteroposterior | 17.69 ± 1.21 | 14.74 ± 1.68 | |
| Cortical bone width (mm) | | | group x plane[4,5] |
| Lateral | 5.84 ± 1.34 | 7.59 ± 0.91 | |
| Medial | 3.85 ± 0.64 | 5.72 ± 0.62 | |
| Anterior | 4.03 ± 0.50 | 5.50 ± 0.48 | |
| Posterior | 4.55 ± 1.19 | 8.54 ± 1.08 | |
| Endosteal bone width (mm) | | | group x plane[6] |
| Lateral | 1.28 + 0.44 | 1.31 ± 0.41 | |
| Medial | 1.02 + 0.24 | 1.21 ± 0.21 | |
| Anterior | 1.17 ± 0.37 | 1.22 ± 0.40 | |
| Posterior | 2.23 ± 0.88 | 1.48 ± 0.57 | |

Group effect: [1]SCI < CON, P = 0.057, $\eta^2 = 0.132$; [2]SCI < CON, P < 0.05

Plane effect: [3]anteroposterior > mediolateral

Group x plane effect: [4]lateral and posterior > medial and anterior in CON; [5]lateral > medial and anterior in SCI: [6]posterior > lateral, medial and anterior sites in SCI but not CON

Table 4.3. Bone area, bone mineral content (BMC) and areal bone mineral density (aBMD) in men with spinal cord injury (SCI) vs controls (CON)

| | SCI (n = 7) | CON (n = 8) |
|---|---|---|
| Mid-femur | | |
| Bone area ($cm^2$) | 43.0 ± 4.5 | 41.8 ± 3.2 |
| BMC (g) | 63.6 ± 10.4[1] | 78.8 ± 10.5 |
| aBMD ($g/cm^2$) | 1.469 ± 0.112[1] | 1.881 ± 0.166 |
| vBMD ($g/cm^3$) | 0.681 ± 0.080[1] | 0.813 ± 0.056 |
| Cort vBMD ($g/cm^3$) | 1.178 ± 0.120 | 1.148 ± 0.055 |
| Arms | | |
| Bone area ($cm^2$) | 501 ± 53 | 491 ± 54 |
| BMC (g) | 441 ± 62 | 407 ± 59 |
| aBMD ($g/cm^2$) | 0.881 ± 0.104 | 0.828 ± 0.059 |

[1]Different from CON, $P < 0.05$

Table 4.4. Measures of bone strength in men with spinal cord injury (SCI) vs controls (CON)

| | SCI (n = 7) | Control (n = 8) | Effect |
|---|---|---|---|
| CSMI ($cm^4$) | | | group, plane |
| mediolateral | 38.1 ± 8.6 | 49.2 ± 15.1 | |
| anteroposterior | 45.3 ± 12.7 | 71.3 ± 17.0 | |
| Polar moment of inertia ($cm^4$) | | | group, plane |
| mediolateral | 4.76 ± 1.08 | 6.15 ± 1.89 | |
| anteroposterior | 5.67 ± 1.59 | 8.91 ± 2.13 | |
| Polar section modulus ($cm^3$) | | | group, plane |
| mediolateral | 3.42 ± 0.59 | 4.24 ± 0.93 | |
| anteroposterior | 3.79 ± 0.80 | 5.60 ± 1.00 | |
| Bone strength index ($g/cm^3$ x $cm^4$) | | | group, plane |
| mediolateral | 44.1 ± 6.2 | 57.1 ± 20.0 | |
| anteroposterior | 53.3 ± 16.6 | 82.4 ± 23.2 | |

Group effect: SCI < CON

Plane effect: mediolateral < anteroposterior

CSMI = cross-sectional moment of inertia

Chapter V

# ASSESSMENT OF SKELETAL MUSCLE MASS IN MEN WITH SPINAL CORD INJURY USING DUAL-ENERGY X-RAY ABSORPTIOMETRY AND MAGNETIC RESONANCE IMAGING

---

Modlesky, Christopher M., Christopher S. Bickel, Jill Slade and Gary A. Dudley

To be submitted to *Journal of Applied Physiology*

Abstract

Some models that estimate skeletal muscle from dual-energy-X-ray absorptiometry (DXA) assume that muscle represents all, or a certain proportion, of the fat-free soft tissue mass (FFST). The purpose of the study was to determine if the proportion of skeletal muscle in the FFST is the same in men with complete SCI (n = 8), 2.3 to 20 years post injury, and healthy men without SCI (n = 8). Skeletal muscle mass of the mid–thigh was determined using magnetic resonance imaging (MRI). FFST was determined in the same region using a total body DXA scan. There were no differences in age, height or weight between the two groups. While men with SCI had lower muscle mass (1.36 ± 0.77 vs 2.44 ± 0.47) and FFST (1.70 ± 0.94 kg vs 2.73 ± 0.80 kg) in the mid-thigh than controls, the proportion of muscle in the FFST of SCI subjects was lower than in controls (0.796 ± 0.094 vs 0.914 ± 0.102, respectively; $P < 0.05$). Despite the discrepancy between the SCI group and controls, strong relationships between mid-thigh muscle and FFST ($r = 0.99$, $P < 0.05$) and the lack of difference in the intercept in the regression of FFST against muscle mass in the SCI group suggests the proportion of muscle in the FFST was consistent and predictable A slope different from one and an intercept different from zero in the controls suggests the prediction of skeletal muscle using DXA may be more complex in young healthy men. The findings suggest there is a disproportionate loss of skeletal muscle after SCI relative to other non-fat constituents. DXA holds promise as a method for assessing skeletal muscle in men who are healthy or with SCI, but it may be influenced by varying levels of adiposity and physical activity.

INDEX WORDS**:** atrophy, body composition, DXA, MRI

## Introduction

Skeletal muscle is the largest component within the fat-free mass, representing approximately 50 % of the non-fat component (6). Accurate quantification of skeletal muscle is important in the assessment of nutritional status, disease risk and physical function (8), as well as the atrophic effects of aging and muscle-wasting diseases. Moreover, understanding the accuracy of methodologies used to assess skeletal muscle allows for better interpretation of muscle status and its response to intervention. Because skeletal muscle in the thighs represents the largest proportion of the total skeletal muscle mass (9), and the connection between body tissue composition and diseases such as osteoporosis appear to be site specific (10), accurate assessment of thigh skeletal muscle is of particular interest.

Magnetic resonance imaging (MRI) provides remarkably accurate estimates of skeletal muscle *in vivo*, rivaled only by quantitative computed tomography (QCT). Studies of human cadavers have demonstrated the validity of MRI and QCT in the assessment of regional skeletal muscle (12). Despite their accuracy, the expense of MRI and QCT and the high radiation exposure associated with QCT precludes their routine use in research and clinical practice. Hence, these reference methodologies are often used to assess the accuracy of less direct but more accessible techniques, such as dual-energy X-ray absorptiometry (DXA).

Some models used to assess skeletal muscle from DXA assume skeletal muscle represents a certain proportion of the fat-free soft tissue mass (FFST) (14) or virtually the entire FFST (9). The few studies that have assessed the validity of DXA using MRI or QCT as the criterion method suggest DXA can provide valid estimates of skeletal muscle

in the limbs (11, 14, 17). However, these studies were conducted primarily in healthy adults. The accuracy of skeletal muscle estimates from DXA may be compromised in disease states and conditions associated with extreme muscle atrophy, such as spinal cord injury (SCI). This notion is supported by a recent report in which the ratio of skeletal muscle to adipose tissue free mass was lower in men with AIDS, a condition associated with extreme muscle atrophy, than healthy controls (19). To our knowledge, no studies have tested whether a similar phenomenon exists in the thigh of men with complete SCI. There is a dramatic reduction in the CSA of skeletal muscle in the thighs after SCI (5). If there is indeed a lower proportion of skeletal muscle in the thighs relative to FFST in individuals with SCI, muscle mass would be overestimated by models that assume muscle represents all or a certain proportion of the FFST.

Thus, the purpose of the present study was to determine if the proportion of skeletal muscle, assessed using MRI, in the FFST from DXA ($FFST_{DXA}$) is similar in the mid-thigh of men with complete and long-standing SCI and able-bodied men of similar age, height and weight. We hypothesized that muscle assessed using MRI would represent a smaller proportion of the $FFST_{DXA}$ in the mid-thigh would be lower in men with SCI.

## Methods

### *Subjects*

Men with complete SCI at the C6-L1 level (n = 8) and at least 2 years post injury were recruited for the study from the Shepherd Center, Atlanta, GA. Healthy men of similar age, height and weight (n = 8) to the SCI individuals were recruited from the

general population. None of the subjects had a history of chronic medication use. The study was approved by the University's Institutional Review Board and written consent was given before testing.

*Magnetic Resonance Imaging*

Approximately 25 axial T1 weighted images of the mid-thigh (1 cm thick separated by 0.5 cm) were collected on a GE 1.5 Tesla magnetic resonance imager using a whole body coil (TR/TE 500/14 20-24 FOV, 1 NEX, 256 x 256 matrix). Images were downloaded to CD and those at the level of the mid-femur (~10 images/subject) were analyzed on a PC using (developed by Ronald Meyer, PhD). Pixels were separated into four different categories (ie, bone, skin, skeletal muscle and adipose tissue) based on signal intensity and anatomical location. After removal of bone and skin pixels from the analysis, pixels with intermediate and high signal intensity were defined as muscle and fat, respectively. Muscle pixels were summed to determine its CSA. Muscle was quantified by multiplying each slice by 1.5 to account for the 1.0 cm slice thickness of each image and the 0.5 cm gap between images. To maintain consistency, all images were analyzed by a single investigator.

*Dual-energy X-ray Absorptiometry*

The total body was scanned using DXA (Delphi A; Hologic, Inc). After completion of the scan, fat, FFST and %Fat were quantified using standard analysis procedures. The scan was then reanalyzed twice to quantify the FFST in the mid-thigh. The mid-thigh was defined by first measuring the length of the right femur from the top

of the femoral head to the bottom of the femoral condyle using the line that dissects the right femoral neck and is one of three lines that surround the pelvis in a triangular fashion. The line was then moved to include the top of the mid thigh and all thigh and leg tissue below that region. After reanalysis, the line was moved to include the bottom of the mid-thigh and all thigh and leg tissue below that region and again reanalyzed. The difference between FFST from the first and second reanalyses was defined as mid-thigh $FFST_{DXA}$.

A calibration step wedge, consisting of thermoplastic resin (68% fat) and thermoplastic resin-aluminum (-10% fat) steps calibrated against stearic acid (100% fat) and water (8.6% fat; Hologic, Inc.) was scanned prior to testing to calibrate fat mass and FFST. Quality control was checked before each test session by scanning a lumbar spine phantom consisting of calcium hydroxyapatite embedded in a cube of thermoplastic resin (model DPA/QDR-1; Hologic x-caliber anthropometric spine phantom). The coefficient of variation of the phantom aBMD during the 3-month period of testing was 0.36%. To ensure consistency, one trained technician performed and analyzed all scans.

*Physical Activity*

Physical activity was assessed in the controls using the 7-day physical activity recall (3). Physical activity levels were determined by using specific MET values for reported activities (1).

*Statistics*

Independent t-tests were used to determine if groups differed in general physical characteristics, total body %Fat, skeletal muscle mass, $FFST_{DXA}$ or the ratio of muscle mass from MRI to $FFST_{DXA}$. Regression analysis was used to determine the relationship between FSST and skeletal muscle mass. Part correlations were used to determine the effect of %Fat and physical activity on differences between muscle mass from MRI and $FFST_{DXA}$ in the mid-thigh. All data were analyzed using SPSS, version 11.0.

Results

Physical characteristics of the two groups are reported in Table 5.1. There were no differences in age, height or weight between the two groups, but SCI had higher total body and mid-thigh %Fat from DXA than controls. Mid-thigh $FFST_{DXA}$ and muscle mass from MRI were both substantially lower in the SCI group than controls (39.7 % and 44.3 %, respectively; $P < 0.05$), but the ratio of muscle mass from MRI to $FFST_{DXA}$ was lower in SCI than CON (12.9 %; $P < 0.05$) suggesting that the SCI group had a lower proportion of muscle in $FFST_{DXA}$.

Despite the difference in the proportion of muscle in the $FFST_{DXA}$, the relationship between $FFST_{DXA}$ and muscle mass from MRI was excellent in the SCI group ($r = 0.99$) and controls ($r = 0.96$) alone (Figure 5.1), and when the groups were combined ($r = 0.96$; $P < 0.05$). Interestingly, visual inspection of Figure 5.1 indicates an intersection the regression lines for the men with SCI and controls at higher levels of muscle mass. The slope of the regression line was different from one in the men with SCI (0.808; $P < 0.05$) and controls (0.568; $P < 0.05$). While the intercept was not

different from zero in the men with SCI (-11; $P < 0.05$), it was greater than zero in the controls (885; $P < 0.05$).

There was a positive relationship between the difference in muscle mass from MRI and $FFST_{DXA}$ and muscle mass from MRI in men with SCI and controls ($r = 0.71$ and 0.79, respectively, $P < 0.05$) suggesting that muscle represented a smaller proportion of the $FFST_{DXA}$ in subjects with higher levels of muscle mass. However, these relationships were reduced and no longer statistically significant when mid-thigh %Fat was included in the regression model (part $r = 0.50$ in men with SCI and 0.35 in controls, $P > 0.05$). In the controls, the relationship was also reduced when physical activity (mean ± SD, 59 ± 69 METs) was included in the regression model with muscle mass from MRI (part $r = 0.58$, $P > 0.05$) and virtually zero when mid-thigh %Fat and physical activity were both included in the regression model (part $r = 0.07$, $P > 0.05$).

## Discussion

To our knowledge, this is the first study to compare skeletal muscle mass from MRI with $FFST_{DXA}$ in men with complete SCI. The major finding was that mid-thigh skeletal muscle represented a significantly smaller proportion of the $FFST_{DXA}$ in men with SCI than controls. This suggests that previous studies using DXA to estimate muscle mass in men with SCI may have underestimated the degree of muscle atrophy associated with SCI (15). Despite the lower proportion of muscle in the $FFST_{DXA}$ in the sample of men with SCI, as indicated by a lower ratio of muscle from MRI to $FFST_{DXA}$ and a slope lower than one when $FFST_{DXA}$ was regressed against muscle mass from MRI (slope = 0.808, $P < 0.05$), $FFST_{DXA}$ and skeletal muscle from MRI were very strongly

related (r = 0.99). Moreover, the intercept was not different from zero. Together, these observations suggest that the proportion of muscle in $FFST_{DXA}$ in men with long-standing SCI is consistent and that regression equations can be developed to estimate skeletal muscle using DXA. Although the relationship between mid-thigh $FFST_{DXA}$ and skeletal muscle from MRI were also strongly correlated in controls (r = 0.96), the significant difference in the slope from one (0.568, $P < 0.05$) and the intercept from zero (885, $P < 0.05$) suggests that prediction of mid-thigh skeletal muscle mass from DXA may be more complex in young healthy men than men with SCI.

Few studies have assessed the proportion of skeletal muscle in the non-fat component of individuals with extreme atrophy. Wang et al. (19) observed a lower ratio of muscle in the adipose tissue-free mass in AIDS patients yielding results similar to the present study. However, the proportion of skeletal muscle in specific regions of the body was not assessed. Following SCI, the decline in skeletal muscle is rapid and limited almost exclusively to the lower limbs (15). Furthermore, Wang et al did not assess the consistency of the ratio. Regression provides a better assessment of the proportionality of skeletal muscle in the $FFST_{DXA}$ than a simple ratio. The slope lower than one and the intercept not different from zero in the present study suggests the proportion of skeletal muscle in min-thigh $FFST_{DXA}$ is consistent and predictable in men with complete and long-standing SCI . Models that accurately quantify skeletal muscle using $FFST_{DXA}$ need to be developed for groups with muscle wasting conditions.

The finding that mid-thigh $FFST_{DXA}$ and muscle mass from MRI were very highly correlated (r = 0.96 to 0.99) is consistent with a prior observation in elderly men and women, in which muscle mass was quantified in the leg, the thigh and the mid thigh

using DXA and CT ($R^2$ = 0.86 to 0.96) (17). The observation that the difference between $FFST_{DXA}$ and mid-thigh muscle mass was positively related to muscle mass in the men with SCI and controls (r = 0.71 and 0.79, respectively, $P < 0.05$) is also consistent with Visser's study with elderly subjects (17). However, in the latter study, the relationship disappeared when several outliers were removed from the analysis. The positive relationship observed in the present study is difficult to explain, but the reduction in the relationship in the men with SCI and controls when mid-thigh %Fat was included in the regression model suggests varying levels of adipose tissue was a contributing factor. Because the relationship also was reduced in the controls when physical activity was included in the regression model with muscle mass from MRI, varying levels of physical activity may have been a contributing factor in the controls. Since approximately 20 % of adipose tissue is comprised of nonfat components, such as water, protein and mineral (18), varying levels of adipose tissue can alter the contribution of skeletal muscle to the $FFST_{DXA}$. Moreover, it is possible that hypertrophy associated with some physical activities may increase the contribution of skeletal muscle to the $FFST_{DXA}$. The limited sample size, however, makes a definitive conclusion tenuous.

If the proportion of skeletal muscle in the $FFST_{DXA}$ does vary with physical activity level, it may effect the ability of DXA to accurately track the changes in skeletal muscle immediately following SCI and in response to exercise intervention. The cross-sectional area of some muscles reduces by more than 50 % within 6 months of injury (3), whereas intervention strategies, such as electrical stimulation of the thigh, have been shown to elicit 20 % increases in the *m.* quadriceps femoris in men with SCI after only 8 weeks (7). It is currently unknown if such rapid increases in skeletal mass can be

accurately detected by DXA. If DXA can predict changes in skeletal muscle following SCI, it would prove to be a powerful, but practical, tool in research and clinical settings.

Because of the coordinating actions of muscle and bone and the positive relationship between these companion tissues, there is a growing interest in determining the extent of their co-dependence. If DXA is found to provide accurate assessment of skeletal muscle during the period of severe atrophy immediately after SCI and during subsequent intervention, it would allow for better study of the relationship between muscle and bone parameters provided by DXA, such as areal bone mineral density (aBMD) and bone mineral content (BMC). In addition to extreme atrophy of skeletal muscle, men with SCI have approximately 20 % less aBMD and BMC in the mid-thigh (13). Moreover, substantial increases in aBMD have been observed in individuals with SCI in response to electrical stimulation intervention (2). Since aBMD is the single best surrogate of fracture risk widely available (4, 16), understanding its link to changes in skeletal muscle would further our understanding of skeletal muscle's role in the maintenance of adequate skeletal health.

In summary, skeletal muscle represents a smaller proportion of the $FFST_{DXA}$ in men with long-standing SCI. This suggests that studies using DXA as a surrogate of skeletal muscle may underestimate muscle atrophy associated with SCI. However, because of the very strong relationship between $FFST_{DXA}$ and mid-thigh muscle mass and the consistency of the proportion of skeletal muscle in the $FFST_{DXA}$ of men with complete and long-standing SCI, DXA holds promise as a method for assessing skeletal muscle status in individuals with extreme muscle atrophy. However, whether DXA can accurately assess changes in skeletal muscle immediately following SCI and in response

to intervention requires further investigation. Future studies examining the potential effect of physical activity on the proportionality of skeletal muscle in the $FFST_{DXA}$ of young healthy men are also needed.

References

1. Ainsworth, B. E., W. L. Haskell, A. S. Leon, D. R. Jacobs, Jr., H. J. Montoye, J. F. Sallis, and R. S. Paffenbarger, Jr. Compendium of physical activities: classification of energy costs of human physical activities. *Med Sci Sports Exerc* 25: 71-80., 1993.

2. Belanger, M., R. B. Stein, G. D. Wheeler, T. Gordon, and B. Leduc. Electrical stimulation: can it increase muscle strength and reverse osteopenia in spinal cord injured individuals? *Arch Phys Med Rehabil* 81: 1090-8., 2000.

3. Blair, S. N., W. L. Haskell, P. Ho, R. S. Paffenbarger, K. M. Vranizan, J. W. Farquhar, and P. D. Wood. Assessment of habitual physical activity by a seven-day recall in a community survey and controlled experiments. *no* 122 (5): 794-804, 1985.

4. Carter, D. R., and W. C. Hayes. The compressive behavior of bone as a two-phase porous structure. *J Bone Joint Surg [Am]* 59: 954-62, 1977.

5. Castro, M. J., D. F. Apple, Jr., E. A. Hillegass, and G. A. Dudley. Influence of complete spinal cord injury on skeletal muscle cross- sectional area within the first 6 months of injury. *Eur J Appl Physiol* 80: 373-8, 1999.

6. Clarys, J. P., A. D. Martin, and D. T. Drinkwater. Gross tissue weights in the human body by cadaver dissection. *Hum Biol* 56: 459-73., 1984.

7. Dudley, G. A., M. J. Castro, S. Rogers, and D. F. Apple, Jr. A simple means of increasing muscle size after spinal cord injury: a pilot study. *Eur J Appl Physiol* 80: 394-6, 1999.

8. Forbes, G. B. *Human body composition: Growth, Aging, Nutrition and Activity*. London: Springer-Verlag, 1987.

9. Heymsfield, S. B., R. Smith, M. Aulet, B. Bensen, S. Lichtman, J. Wang, and R. N. Pierson, Jr. Appendicular skeletal muscle mass: measurement by dual-photon absorptiometry. *Am J Clin Nutr* 52: 214-8., 1990.

10. Kerr, D., A. Morton, I. Dick, and R. Prince. Exercise effects on bone mass in postmenopausal women are site-specific and load-dependent. *J Bone Miner Res* 11: 218-225, 1996.

11. Levine, J. A., L. Abboud, M. Barry, J. E. Reed, P. F. Sheedy, and M. D. Jensen. Measuring leg muscle and fat mass in humans: comparison of CT and dual- energy X-ray absorptiometry. *J Appl Physiol* 88: 452-6., 2000.

12. Mitsiopoulos, N., R. N. Baumgartner, S. B. Heymsfield, W. Lyons, D. Gallagher, and R. Ross. Cadaver validation of skeletal muscle measurement by magnetic resonance imaging and computerized tomography. *J Appl Physiol* 85: 115-22., 1998.

13. Modlesky, C. M., J. Slade, S. B. Bickel, and G. A. Dudley. The effect of unloading on bone structure and strength in men with complete spinal cord injury. *Bone* , In preparation.

14. Shih, R., Z. Wang, M. Heo, W. Wang, and S. B. Heymsfield. Lower limb skeletal muscle mass: development of dual-energy X-ray absorptiometry prediction model. *J Appl Physiol* 89: 1380-6., 2000.

15. Spungen, A. M., J. Wang, R. N. Pierson, Jr., and W. A. Bauman. Soft tissue body composition differences in monozygotic twins discordant for spinal cord injury. *J Appl Physiol* 88: 1310-5., 2000.

16. Turner, C. H. Yield behavior of bovine cancellous bone [published erratum appears in J Biomech Eng 1989 Nov;111(4):335]. *J Biomech Eng* 111: 256-60, 1989.

17. Visser, M., T. Fuerst, T. Lang, L. Salamone, and T. B. Harris. Validity of fan-beam dual-energy X-ray absorptiometry for measuring fat- free mass and leg muscle mass. Health, Aging, and Body Composition Study--Dual-Energy X-ray Absorptiometry and Body Composition Working Group. *J Appl Physiol* 87: 1513-20., 1999.

18. Wang, J., and R. N. Pierson, Jr. Disparate hydration of adipose and lean tissue require a new model for body water distribution in man. *J Nutr* 106: 1687-93., 1976.

19. Wang, Z., M. Heo, R. C. Lee, D. P. Kotler, R. T. Withers, and S. B. Heymsfield. Muscularity in adult humans: proportion of adipose tissue-free body mass as skeletal muscle. *Am J Human Biol* 13: 612-9., 2001.

Table 5.1. Physical characteristics of men with spinal cord injury (SCI) and controls (CON)

| | SCI (n = 8) | CON (n = 8) |
|---|---|---|
| Age (y) | 35 ± 9 | 33 ± 9 |
| Height (cm) | 179.7 ± 8.0 | 177.4 ± 7.4 |
| Weight (kg) | 79.6 ± 19.9 | 78.7 ± 20.7 |
| Mid-thigh | | |
| %Fat | 33.8 ± 16.4* | 16.2 ± 8.7 |
| Fat-free soft tissue (kg) | 1.696 ± 0.943* | 2.733 ± 0.796 |
| Muscle mass (kg) | 1.358 ± 0.772* | 2.438 ± 0.471 |
| Muscle/FFST | 0.796 ± 0.094* | 0.914 ± 0.102 |

*Different from CON, $P < 0.05$. Mid-thigh %Fat and fat-free soft tissue were determined using dual-energy X-ray absorptiometry. Muscle mass was determined using magnetic resonance imaging.

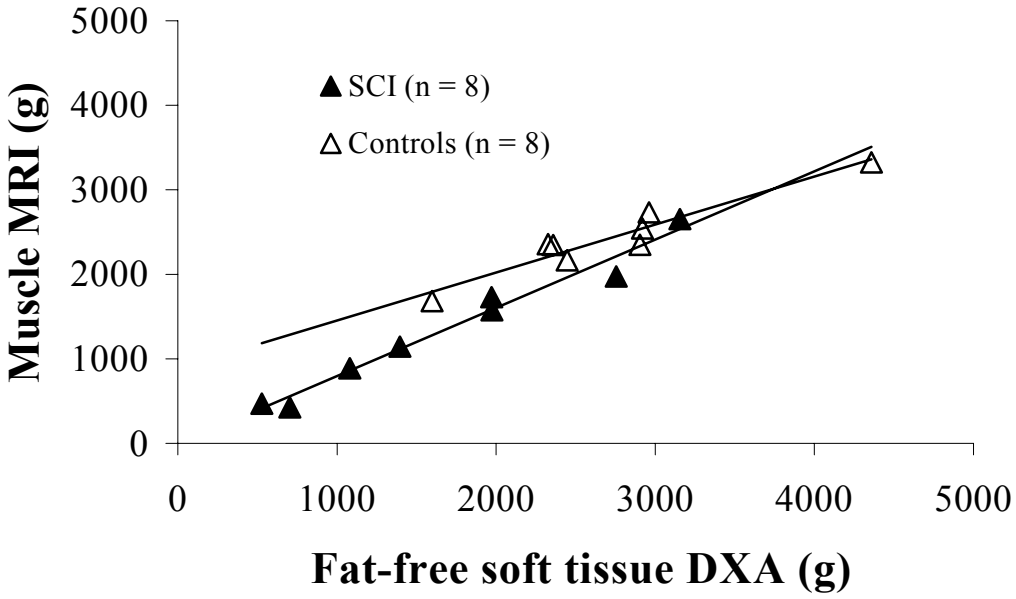


Figure 5.1. Relationship between fat-free soft tissue mass from dual-energy X-ray absorptiometry ($FFST_{DXA}$ ) and skeletal muscle mass from magnetic resonance imaging in men with spinal cord injury (SCI) (muscle from MRI (g) = 0.808 * $FFST_{DXA}$ (g) – 11.4; r = 0.99) and controls (muscle MRI (g) = 0.568 * $FFST_{DXA}$ (g) + 885; r = 0.96).

# Chapter VI

## SUMMARY

Several studies have demonstrated drastic deterioration of aBMD and BMC in the lower limbs after SCI.. However, most of these studies ignored the effect of extreme unloading on bone quality. The oversight was largely due to technological limitations. Using advanced technology with high resolution magnetic resonance imaging it was discovered that men with SCI also have deteriorated trabecular bone microarchitecture in the distal femur and proximal tibia, two frequent fracture sites. Such a finding has biological significance because of the notion that deteriorated trabeculae can not be recovered. It is also of clinical significance because of the marked increase in fracture incidence about the knee SCI. Moreover, it underscores the powerful effect of ambulation and general physical function in the maintenance of skeletal tissue quality.

In addition to the deterioration of the microarchitectural aspects of trabecular bone, it was found that the macroarchitecture, or structure, of the mid-femur was impaired in men with SCI. The structural deterioration was accompanied by markedly lower bending and torsional strength. Although the latter finding does not correspond with some prior studies, it is congruent with the marked increase in fracture incidence in the femoral shaft after injury. It is plausible that the use of magnetic resonance imaging in the present study yielded a more accurate representation of the bone strength impairment associated with SCI.

Using MRI it was also discovered that men with SCI have a lower proportion of skeletal muscle in the FFST of the mid-thigh than assumed by some DXA models of skeletal muscle assessment. Thus, regression equations, specific to conditions that cause extreme muscle atrophy in the lower limbs, may need to be developed to accurately asses skeletal muscle in individuals with SCI. Additional studies are needed to determine if DXA can accurately assess the rapid atrophy after SCI and hypertrophy associated with intervention.

LITERATURE CITED

1. Ainsworth, B. E., W. L. Haskell, A. S. Leon, D. R. Jacobs, Jr., H. J. Montoye, J. F. Sallis, and R. S. Paffenbarger, Jr. Compendium of physical activities: classification of energy costs of human physical activities. *Med Sci Sports Exerc* 25: 71-80., 1993.

2. Baron, R. Anatomy and untrastructure of bone. In: *Primer and Metabolic Diseases and Disorders of Mineral Metabolism* (4 ed.), edited by M. J. Farvus. Phil: Lippincott Williams & Wilkins, 1999, p. 3-10.

3. Belanger, M., R. B. Stein, G. D. Wheeler, T. Gordon, and B. Leduc. Electrical stimulation: can it increase muscle strength and reverse osteopenia in spinal cord injured individuals? *Arch Phys Med Rehabil* 81: 1090-8., 2000.

4. Bergot, C., A. M. Laval-Jeantet, K. Hutchinson, I. Dautraix, F. Caulin, and H. K. Genant. A comparison of spinal quantitative computed tomography with dual energy X-ray absorptiometry in European women with vertebral and nonvertebral fractures. *Calcif Tissue Int* 68: 74-82., 2001.

5. Bergula, A. P., W. Huang, and J. A. Frangos. Femoral vein ligation increases bone mass in the hindlimb suspended rat. *Bone* 24: 171-7., 1999.

6. Beuf, O., S. Ghosh, D. C. Newitt, T. M. Link, L. Steinbach, M. Ries, N. Lane, and S. Majumdar. Magnetic resonance imaging of normal and osteoarthritic trabecular bone structure in the human knee. *Arthritis Rheum* 46: 385-93., 2002.

7. Biering-Sorensen, F., H. Bohr, and O. Schaadt. Bone mineral content of the lumbar spine and lower extremities years after spinal cord lesion. *Paraplegia* 26: 293-301, 1988.

8. Biering-Sorensen, F., H. H. Bohr, and O. P. Schaadt. Longitudinal study of bone mineral content in the lumbar spine, the forearm and the lower extremities after spinal cord injury. *Eur J Clin Invest* 20: 330-5, 1990.

9. Blair, S. N., W. L. Haskell, P. Ho, R. S. Paffenbarger, K. M. Vranizan, J. W. Farquhar, and P. D. Wood. Assessment of habitual physical activity by a seven-day recall in a community survey and controlled experiments. *no* 122 (5): 794-804, 1985.

10. Bourrin, S., S. Palle, C. Genty, and C. Alexandre. Physical exercise during remobilization restores a normal bone trabecular network after tail suspension-induced osteopenia in young rats. *J Bone Miner Res* 10: 820-8, 1995.

11. Bouxsein, M. L., B. S. Coan, and S. C. Lee. Prediction of the strength of the elderly proximal femur by bone mineral density and quantitative ultrasound measurements of the heel and tibia. *Bone* 25: 49-54., 1999.

12. Carter, D. R., and W. C. Hayes. The compressive behavior of bone as a two-phase porous structure. *J Bone Joint Surg [Am]* 59: 954-62, 1977.

13. Castro, M. J., D. F. Apple, Jr., E. A. Hillegass, and G. A. Dudley. Influence of complete spinal cord injury on skeletal muscle cross- sectional area within the first 6 months of injury. *Eur J Appl Physiol* 80: 373-8, 1999.

14. Castro, M. J., D. F. Apple, Jr., R. S. Staron, G. E. Campos, and G. A. Dudley. Influence of complete spinal cord injury on skeletal muscle within 6 mo of injury. *J Appl Physiol* 86: 350-8, 1999.

15. Christiansen, C., M. S. Christensen, P. McNair, C. Hagen, K. E. Stocklund, and I. Transbol. Prevention of early postmenopausal bone loss: controlled 2-year study in 315 normal females. *Eur J Clin Invest* 10: 273-9, 1980.

16. Chung, H. W., F. W. Wehrli, J. L. Williams, and S. L. Wehrli. Three-dimensional nuclear magnetic resonance microimaging of trabecular bone. *J Bone Miner Res* 10: 1452-61., 1995.

17. Ciarelli, T. E., D. P. Fyhrie, M. B. Schaffler, and S. A. Goldstein. Variations in three-dimensional cancellous bone architecture of the proximal femur in female hip fractures and in controls. *J Bone Miner Res* 15: 32-40, 2000.

18. Clarys, J. P., A. D. Martin, and D. T. Drinkwater. Gross tissue weights in the human body by cadaver dissection. *Hum Biol* 56: 459-73., 1984.

19. Collet, P., D. Uebelhart, L. Vico, L. Moro, D. Hartmann, M. Roth, and C. Alexandre. Effects of 1- and 6-month spaceflight on bone mass and biochemistry in two humans. *Bone* 20: 547-51, 1997.

20. Comarr, E., R. Hutchinson, and E. Bors. Extremity fractures of patients with spinal cord injuries. *Am J Surg* 103: 732-739, 1962.

21. Dawson-Hughes, B. Calcium and vitamin D nutritional needs of elderly women. *J Nutr* 126: 1165S-1167S, 1996.

22. de Bruin, E. D., P. Frey-Rindova, R. E. Herzog, V. Dietz, M. A. Dambacher, and E. Stussi. Changes of tibia bone properties after spinal cord injury: effects of early intervention. *Arch Phys Med Rehabil* 80: 214-20, 1999.

23. de Bruin, E. D., R. Herzog, R. H. Rozendal, D. Michel, and E. Stussi. Estimation of geometric properties of cortical bone in spinal cord injury. *Arch Phys Med Rehabil* 81: 150-6., 2000.

24. Dempster, D. W. The contribution of trabecular architecture to cancellous bone quality [editorial]. *J Bone Miner Res* 15: 20-3, 2000.

25. Dodd, J. S., J. A. Raleigh, and T. S. Gross. Osteocyte hypoxia: a novel mechanotransduction pathway. *Am J Physiol* 277: C598-602., 1999.

26. Dudley, G. A., M. J. Castro, S. Rogers, and D. F. Apple, Jr. A simple means of increasing muscle size after spinal cord injury: a pilot study. *Eur J Appl Physiol* 80: 394-6, 1999.

27. Duncan, C. S., C. J. Blimkie, A. Kemp, W. Higgs, C. T. Cowell, H. Woodhead, J. N. Briody, and R. Howman-Giles. Mid-femur geometry and biomechanical properties in 15- to 18-yr-old female athletes. *Med Sci Sports Exerc* 34: 673-81., 2002.

28. Einhorn, T. A. Biomechanics of bone. In: *Principles of Bone Biology*, edited by J. P. Bilezikian, Raisz, L.G., Rodan, G.A. San Diego: Academic Press, 1996, p. 25-37.

29. Ferretti, J. L., R. F. Capozza, and J. R. Zanchetta. Mechanical validation of a tomographic (pQCT) index for noninvasive estimation of rat femur bending strength. *Bone* 18: 97-102., 1996.

30. Forbes, G. B. *Human body composition: Growth, Aging, Nutrition and Activity*. London: Springer-Verlag, 1987.

31. Freehafer, A. A. Limb fractures in patients with spinal cord injury. *Arch Phys Med Rehabil* 76: 823-7, 1995.

32. Garber, M. A., D. L. McDowell, and W. C. Hutton. Bone loss during simulated weightlessness: a biomechanical and mineralization study in the rat model. *Aviat Space Environ Med* 71: 586-92., 2000.

33. Garland, D. E., C. A. Stewart, R. H. Adkins, S. S. Hu, C. Rosen, F. J. Liotta, and D. A. Weinstein. Osteoporosis after spinal cord injury. *J Orthop Res* 10: 371-8, 1992.

34. Giangregorio, L., and C. C. Blimkie. Skeletal adaptations to alterations in weight-bearing activity: a comparison of models of disuse osteoporosis. *Sports Med* 32: 459-76, 2002.

35. Glaser, R. M. Functional neuromuscular stimulation. Exercise conditioning of spinal cord injured patients. *Int J Sports Med* 15: 142-8, 1994.

36. Go, B. K., M. J. DeVivo, and J. S. Richards. The Epidemiology of Spinal Cord Injury. In: *Spinal Cord Injury: Clinical Outcomes from the Model Systems*, edited by S. L. Stover, DeLisa, J.A., Whiteneck, G.G. Gaithersburg, MD: Aspen Publishers, 1995, p. 21-55.

37. Goemaere, S., M. Van Laere, P. De Neve, and J. M. Kaufman. Bone mineral status in paraplegic patients who do or do not perform standing. *Osteoporos Int* 4: 138-43, 1994.

38. Gordon, T., and J. Mao. Muscle atrophy and procedures for training after spinal cord injury. *Phys Ther* 74: 50-60, 1994.

39. Goulet, R. W., S. A. Goldstein, M. J. Ciarelli, J. L. Kuhn, M. B. Brown, and L. A. Feldkamp. The relationship between the structural and orthogonal compressive properties of trabecular bone. *J Biomech* 27: 375-89, 1994.

40. Greenfield, M. A. Current status of physical measurements of the skeleton. *Med Phys* 19: 1349-57., 1992.

41. Grimby, G., C. Broberg, I. Krotkiewska, and M. Krotkiewski. Muscle fiber composition in patients with traumatic cord lesion. *Scand J Rehabil Med* 8: 37-42, 1976.

42. Heymsfield, S. B., R. Smith, M. Aulet, B. Bensen, S. Lichtman, J. Wang, and R. N. Pierson, Jr. Appendicular skeletal muscle mass: measurement by dual-photon absorptiometry. *Am J Clin Nutr* 52: 214-8., 1990.

43. Hillegass, E. A., and G. A. Dudley. Surface electrical stimulation of skeletal muscle after spinal cord injury. *Spinal Cord* 37: 251-7, 1999.

44. Hipp, J. A., A. Jansujwicz, C. A. Simmons, and B. D. Snyder. Trabecular bone morphology from micro-magnetic resonance imaging. *J Bone Miner Res* 11: 286-97., 1996.

45. Holick, M. F. McCollum Award Lecture, 1994: vitamin D--new horizons for the 21st century. *Am J Clin Nutr* 60: 619-30., 1994.

46. Holick, M. F. Perspective on the impact of weightlessness on calcium and bone metabolism. *Bone* 22: 105S-111S, 1998.

47. Inman, C. L., G. L. Warren, H. A. Hogan, and S. A. Bloomfield. Mechanical loading attenuates bone loss due to immobilization and calcium deficiency. *J Appl Physiol* 87: 189-95, 1999.

48. Ito, M., A. Nishida, T. Nakamura, M. Uetani, and K. Hayashi. Differences of three-dimensional trabecular microstructure in osteopenic rat models caused by ovariectomy and neurectomy. *Bone* 30: 594-8., 2002.

49. Jaworski, Z. F., M. Liskova-Kiar, and H. K. Uhthoff. Effect of long-term immobilisation on the pattern of bone loss in older dogs. *J Bone Joint Surg Br* 62-B: 104-10., 1980.

50. Jones, L. M., A. Goulding, and D. F. Gerrard. DEXA: a practical and accurate tool to demonstrate total and regional bone loss, lean tissue loss and fat mass gain in paraplegia. *Spinal Cord* 36: 637-40, 1998.

51. Kazarian, L. E., and H. E. Von Gierke. Bone loss as a result of immobilization and chelation. Preliminary results in Macaca mulatta. *Clin Orthop* 65: 67-75., 1969.

52. Kerr, D., A. Morton, I. Dick, and R. Prince. Exercise effects on bone mass in postmenopausal women are site-specific and load-dependent. *J Bone Miner Res* 11: 218-225, 1996.

53. Khan, K., H. McKay, P. Kannus, D. Bailey, J. Wark, and K. Bennell. *Physical Activity and Bone Health*. Champaign, IL: Human Kinetics, 2001.

54. Kiratli, B. J., A. E. Smith, T. Nauenberg, C. F. Kallfelz, and I. Perkash. Bone mineral and geometric changes through the femur with immobilization due to spinal cord injury. *J Rehabil Res Dev* 37: 225-33., 2000.

55. Kleerekoper, M., A. R. Villanueva, J. Stanciu, D. S. Rao, and A. M. Parfitt. The role of three-dimensional trabecular microstructure in the pathogenesis of vertebral compression fractures. *Calcif Tissue Int* 37: 594-7, 1985.

56. Klein-Nulend, J., A. van der Plas, C. M. Semeins, N. E. Ajubi, J. A. Frangos, P. J. Nijweide, and E. H. Burger. Sensitivity of osteocytes to biomechanical stress in vitro. *Faseb J* 9: 441-5., 1995.

57. Leblanc, A. D., V. S. Schneider, H. J. Evans, D. A. Engelbretson, and J. M. Krebs. Bone mineral loss and recovery after 17 weeks of bed rest. *J Bone Miner Res* 5: 843-50, 1990.

58. Lee, T. Q., T. A. Shapiro, and D. M. Bell. Biomechanical properties of human tibias in long-term spinal cord injury. *J Rehabil Res Dev* 34: 295-302, 1997.

59. Levine, J. A., L. Abboud, M. Barry, J. E. Reed, P. F. Sheedy, and M. D. Jensen. Measuring leg muscle and fat mass in humans: comparison of CT and dual- energy X-ray absorptiometry. *J Appl Physiol* 88: 452-6., 2000.

60. Levy, M., J. Mizrahi, and Z. Susak. Recruitment, force and fatigue characteristics of quadriceps muscles of paraplegics isometrically activated by surface functional electrical stimulation. *J Biomed Eng* 12: 150-6, 1990.

61. Link, T. M., S. Majumdar, P. Augat, J. C. Lin, D. Newitt, Y. Lu, N. E. Lane, and H. K. Genant. In vivo high resolution MRI of the calcaneus: differences in trabecular structure in osteoporosis patients. *J Bone Miner Res* 13: 1175-82, 1998.

62. Link, T. M., V. Vieth, J. Matheis, D. Newitt, Y. Lu, E. J. Rummeny, and S. Majumdar. Bone structure of the distal radius and the calcaneus vs BMD of the spine and proximal femur in the prediction of osteoporotic spine fractures. *Eur Radiol* 12: 401-8., 2002.

63. Mack, P. B., P. A. LaChance, G. P. Vose, and F. B. Vogt. Bone demineralization of foot and hand of gemini-titan IV, V and VII astronauts during orbital flight. *Am J Roentgenol Radium Ther Nucl Med* 100: 503-11, 1967.

64. Majumdar, S., and H. K. Genant. High resolution magnetic resonance imaging of trabecular structure. *Eur Radiol* 7: S51-5., 1997.

65. Majumdar, S., H. K. Genant, S. Grampp, D. C. Newitt, V. H. Truong, J. C. Lin, and A. Mathur. Correlation of trabecular bone structure with age, bone mineral density, and osteoporotic status: in vivo studies in the distal radius using high resolution magnetic resonance imaging. *J Bone Miner Res* 12: 111-8., 1997.

66. Majumdar, S., M. Kothari, P. Augat, D. C. Newitt, T. M. Link, J. C. Lin, T. Lang, Y. Lu, and H. K. Genant. High-resolution magnetic resonance imaging: three-dimensional trabecular bone architecture and biomechanical properties. *Bone* 22: 445-54, 1998.

67. Majumdar, S., T. M. Link, P. Augat, J. C. Lin, D. Newitt, N. E. Lane, and H. K. Genant. Trabecular bone architecture in the distal radius using magnetic resonance imaging in subjects with fractures of the proximal femur. Magnetic Resonance Science Center and Osteoporosis and Arthritis Research Group. *Osteoporos Int* 10: 231-9, 1999.

68. Majumdar, S., D. Newitt, M. Jergas, A. Gies, E. Chiu, D. Osman, J. Keltner, J. Keyak, and H. Genant. Evaluation of technical factors affecting the quantification of trabecular bone structure using magnetic resonance imaging. *Bone* 17: 417-30, 1995.

69. Majumdar, S., D. Newitt, A. Mathur, D. Osman, A. Gies, E. Chiu, J. Lotz, J. Kinney, and H. Genant. Magnetic resonance imaging of trabecular bone structure in the distal radius: relationship with X-ray tomographic microscopy and biomechanics. *Osteoporos Int* 6: 376-85, 1996.

70. Marcus, R. Mechanisms of exercise effects on bone. In: *Principles of bone biology*, edited by J. P. Bilezikian, Raisz, L.G., Rodan, G.A. San Diego: Academic Press, 1996, p. 1135-1146.

71. Marks, S. C., and D. C. Hermey. The structure and development of bone. In: *Principles of Bone Biology*, edited by J. P. Bilezikian, L. G. Raisz and G. A. Rodan. San Diego: Academic Press, 1996, p. 3-14.

72. Martin, T. P., R. B. Stein, P. H. Hoeppner, and D. C. Reid. Influence of electrical stimulation on the morphological and metabolic properties of paralyzed muscle. *J Appl Physiol* 72: 1401-6, 1992.

73. Mazess, R. B., and G. D. Whedon. Immobilization and bone. *Calcif Tissue Int* 35: 265-7, 1983.

74. Minaire, P., P. Neunier, C. Edouard, J. Bernard, P. Courpron, and J. Bourret. Quantitative histological data on disuse osteoporosis: comparison with biological data. *Calcif Tissue Res* 17: 57-73, 1974.

75. Mitsiopoulos, N., R. N. Baumgartner, S. B. Heymsfield, W. Lyons, D. Gallagher, and R. Ross. Cadaver validation of skeletal muscle measurement by magnetic resonance imaging and computerized tomography. *J Appl Physiol* 85: 115-22., 1998.

76. Modlesky, C. M., J. Slade, S. B. Bickel, and G. A. Dudley. The effect of unloading on bone structure and strength in men with complete spinal cord injury. *Bone* , In preparation.

77. O'Connor, J. A., and L. E. Lanyon. The influence of strain rate on adaptive bone remodelling. *Journal of Biomechanics* 15: 767-781, 1982.

78. Ouyang, X., K. Selby, P. Lang, K. Engelke, C. Klifa, B. Fan, F. Zucconi, G. Hottya, M. Chen, S. Majumdar, and H. K. Genant. High resolution magnetic resonance imaging of the calcaneus: age- related changes in trabecular structure and comparison with dual X-ray absorptiometry measurements. *Calcif Tissue Int* 60: 139-47, 1997.

79. Pacy, P. J., R. H. Evans, and D. Halliday. Effect of anaerobic and aerobic exercise promoted by computer regulated functional electrical stimulation (FES) on muscle size, strength and histology in paraplegic males. *Prosthet Orthot Int* 11: 75-9, 1987.

80. Pacy, P. J., J. Webster, and J. S. Garrow. Exercise and obesity. *Sports Med* 3: 89-113, 1986.

81. Parfitt, A. M. Bone histomorphometry: standardization of nomenclature, symbols and units. Summary of proposed system. *Bone Miner* 4: 1-5., 1988.

82. Parfitt, A. M. Trabecular bone architecture in the pathogenesis and prevention of fracture. *Am J Med* 82: 68-72, 1987.

83. Parfitt, A. M., M. K. Drezner, F. H. Glorieux, J. A. Kanis, H. Malluche, P. J. Meunier, S. M. Ott, and R. R. Recker. Bone histomorphometry: standardization of nomenclature, symbols, and units. Report of the ASBMR Histomorphometry Nomenclature Committee. *J Bone Miner Res* 2: 595-610., 1987.

84. Petit, M. A., H. A. McKay, K. J. MacKelvie, A. Heinonen, K. M. Khan, and T. J. Beck. A randomized school-based jumping intervention confers site and maturity-specific benefits on bone structural properties in girls: a hip structural analysis study. *J Bone Miner Res* 17: 363-72., 2002.

85. Pietschmann, P., P. Pils, W. Woloszczuk, R. Maerk, D. Lessan, and J. Stipicic. Increased serum osteocalcin levels in patients with paraplegia. *Paraplegia* 30: 204-9., 1992.

86. Rabischong, E., and F. Ohanna. Effects of functional electrical stimulation (FES) on evoked muscular output in paraplegic quadriceps muscle. *Paraplegia* 30: 467-73, 1992.

87. Roberts, D., W. Lee, R. C. Cuneo, J. Wittmann, G. Ward, R. Flatman, B. McWhinney, and P. E. Hickman. Longitudinal study of bone turnover after acute spinal cord injury. *J Clin Endocrinol Metab* 83: 415-22, 1998.

88. Rochester, L., M. J. Barron, C. S. Chandler, R. A. Sutton, S. Miller, and M. A. Johnson. Influence of electrical stimulation of the tibialis anterior muscle in paraplegic subjects. 2. Morphological and histochemical properties. *Paraplegia* 33: 514-22, 1995.

89. Rochester, L., C. S. Chandler, M. A. Johnson, R. A. Sutton, and S. Miller. Influence of electrical stimulation of the tibialis anterior muscle in paraplegic subjects. 1. Contractile properties. *Paraplegia* 33: 437-49, 1995.

90. Roer, R. D., and R. M. Dillaman. Bone growth and calcium balance during simulated weightlessness in the rat. *J Appl Physiol* 68: 13-20, 1990.

91. Round, J. M., F. M. Barr, B. Moffat, and D. A. Jones. Fibre areas and histochemical fibre types in the quadriceps muscle of paraplegic subjects. *J Neurol Sci* 116: 207-11, 1993.

92. Rubin, C. T., and L. E. Lanyon. Dynamic strain similarity in vertebrates; an alternative to allometric limb bone scaling. *J Theor Biol* 107: 321-7., 1984.

93. Rubin, C. T., and L. E. Lanyon. Regulation of bone mass by mechanical strain magnitude. *Calcif Tissue Int* 37: 411-417, 1985.

94. Shields, R. K. Fatigability, relaxation properties, and electromyographic responses of the human paralyzed soleus muscle. *J Neurophysiol* 73: 2195-206, 1995.

95. Shih, R., Z. Wang, M. Heo, W. Wang, and S. B. Heymsfield. Lower limb skeletal muscle mass: development of dual-energy X-ray absorptiometry prediction model. *J Appl Physiol* 89: 1380-6., 2000.

96. Spungen, A. M., J. Wang, R. N. Pierson, Jr., and W. A. Bauman. Soft tissue body composition differences in monozygotic twins discordant for spinal cord injury. *J Appl Physiol* 88: 1310-5., 2000.

97. Stein, R. B., T. Gordon, J. Jefferson, A. Sharfenberger, J. F. Yang, J. T. de Zepetnek, and M. Belanger. Optimal stimulation of paralyzed muscle after human spinal cord injury. *J Appl Physiol* 72: 1393-400, 1992.

98. Turner, C. H. Exercising the skeleton: beneficial effects of mechanical loading on bone structure. *Endocrinol* 10: 164-169, 2000.

99. Turner, C. H. Site-specific skeletal effects of exercise: importance of interstitial fluid pressure [comment]. *Bone* 24: 161-2, 1999.

100. Turner, C. H. Yield behavior of bovine cancellous bone [published erratum appears in J Biomech Eng 1989 Nov;111(4):335]. *J Biomech Eng* 111: 256-60, 1989.

101. Turner, C. H., and D. B. Burr. Experimantal techniques for bone mechanics. In: *Bone Mechanics Handbook*, edited by S. C. Cowen. Boca Raton: CRC Press, 2001, p. 1-35.

102. Uebelhart, D., B. Demiaux-Domenech, M. Roth, and A. Chantraine. Bone metabolism in spinal cord injured individuals and in others who have prolonged immobilisation. A review. *Paraplegia* 33: 669-73, 1995.

103. Uhthoff, H. K., and Z. F. Jaworski. Bone loss in response to long-term immobilisation. *J Bone Joint Surg Br* 60-B: 420-9., 1978.

104. Vestergaard, P., K. Krogh, L. Rejnmark, and L. Mosekilde. Fracture rates and risk factors for fractures in patients with spinal cord injury. *Spinal Cord* 36: 790-6, 1998.

105. Vico, L., D. Chappard, S. Palle, A. V. Bakulin, V. E. Novikov, and C. Alexandre. Trabecular bone remodeling after seven days of weightlessness exposure (BIOCOSMOS 1667). *Am J Physiol* 255: R243-7, 1988.

106. Visser, M., T. Fuerst, T. Lang, L. Salamone, and T. B. Harris. Validity of fan-beam dual-energy X-ray absorptiometry for measuring fat- free mass and leg muscle mass. Health, Aging, and Body Composition Study--Dual-Energy X-ray Absorptiometry and Body Composition Working Group. *J Appl Physiol* 87: 1513-20., 1999.

107. Vogel, J., and M. Whittle. Bone mineral changes: the second manned skylab mission. *Aviat Space and Environ Med* 47: 396-400, 1976.

108. Wang, J., and R. N. Pierson, Jr. Disparate hydration of adipose and lean tissue require a new model for body water distribution in man. *J Nutr* 106: 1687-93., 1976.

109. Wang, Z., M. Heo, R. C. Lee, D. P. Kotler, R. T. Withers, and S. B. Heymsfield. Muscularity in adult humans: proportion of adipose tissue-free body mass as skeletal muscle. *Am J Human Biol* 13: 612-9., 2001.

110. Wilmet, E., A. A. Ismail, A. Heilporn, D. Welraeds, and P. Bergmann. Longitudinal study of the bone mineral content and of soft tissue composition after spinal cord section. *Paraplegia* 33: 674-7, 1995.

111. Woodhead, H. J., A. F. Kemp, C. J. R. Blimkie, J. N. Briody, C. S. Duncan, M. Thompson, A. Lam, R. Howman-Giles, and C. T. Cowell. Measurement of midfemoral shaft geometry: repeatability and accuracy using magnetic resonance imaging and dual-energy X-ray absorptiometry. *J Bone Miner Res* 16: 2251-9., 2001.

112. Zerwekh, J. E., L. A. Ruml, F. Gottschalk, and C. Y. Pak. The effects of twelve weeks of bed rest on bone histology, biochemical markers of bone turnover, and calcium homeostasis in eleven normal subjects. *J Bone Miner Res* 13: 1594-601, 1998.